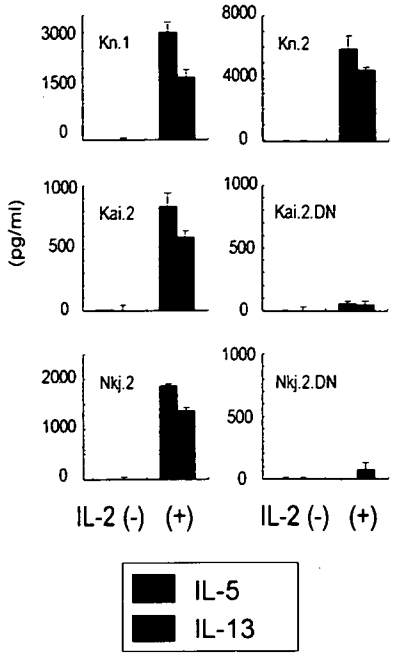

FIGURE 2. Exogenous IL-2 also triggered IL-13 production. $CD4^+$ iNKT cell clones Kn.1, Kai.2, Nkj.2, and Kn.2 as well as DN clones Kai.2. DN and Nkj.2. DN were stimulated with iDCs in the presence of IL-2. Supernatants were collected 48 h later and used for measurement of IL-5 (CBA) and -13 (ELISA). All of the data represent mean cytokine concentration from triplicate samples with error bars indicating +SD.

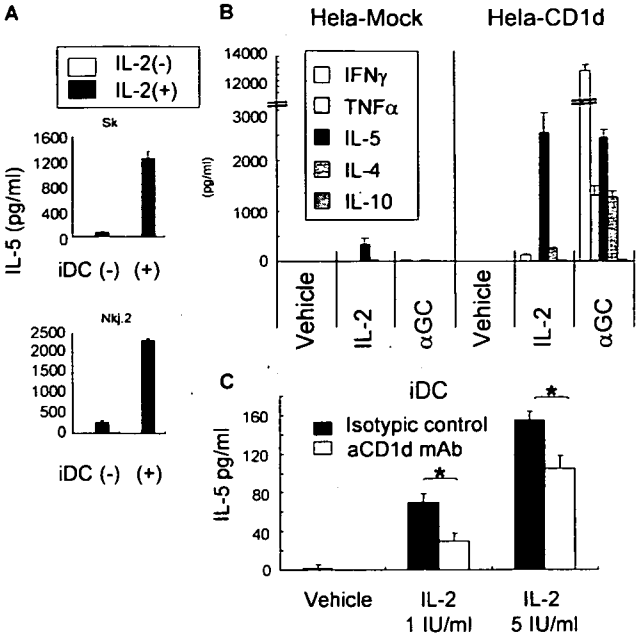

FIGURE 3. TCR-CD1d interaction was required for IL-2-mediated IL-5 production from iNKT clones. *A*, Presence of iDCs is critical for IL-5 production. $CD4^+$ iNKT clone cells Sk and Nkj.2 were cultured with or without iDCs in the presence or absence of IL-2 (10 IU/ml). Cytokines in the supernatant were measured by CBA after 48 h coculture. *B*, Comparison of CD1d- and Mock-transfected HeLa cells for IL-5 induction. The cytokine production of $CD4^+$ iNKT clone cells (Kn.1 and Kn.2) in response to IL-2 (10 IU/ml) and αGC (100 ng/ml) was evaluated by culturing them with CD1d-transfected or mock-transfected HeLa cells. For αGC stimulation, HeLa cells were loaded with αGC or DMSO (vehicle) for 12 h before incubation with iNKT cells. *C*, Suppression of IL-5 production by anti-CD1d blocking Ab. IL-5 production of $CD4^+$ iNKT clone cells (Kai.1 and Kk) in response to IL-2 stimuli (1 IU/ml, 5 IU/ml) was evaluated in the coculture with iDCs. To evaluate the involvement of CD1d, we added anti-CD1d mAb (aCD1d 59; 10 μg/ml) or isotype control Ab from the start of culture. Data represent mean cytokine concentration from triplicate samples with error bars indicating +SD. Although not indicated here, this blocking Ab significantly suppressed IFN-γ production induced by αGC stimulation by the same clones (*, $p < 0.01$, one-factor ANOVA).

donors by the single-cell sorting method, and estimate the frequency of IL-5-producing cells. Although the method is feasible, because it is laborious and time consuming, we selected two donors from whom we could reproducibly generate IL-5-producing clones. We found that two of five single cell-sorted clones derived from one donor efficiently produced IL-5 in response to IL-2. In another donor, the number was one of four (data not shown). This data implies that the frequency of IL-5-producing iNKT cell clones may reach 25–40% of total $CD4^+$ iNKT cells in individuals who have a higher number of IL-5-producing iNKT cells.

IL-15 could replace IL-2 in mediating the IL-5 production

To determine whether any cytokines other than IL-2 could also induce IL-5 production, representative IL-5-producing clones Kn.1, Kai.1, and Kai.2 were stimulated with IL-4, IL-7, IL-9, IL-15, IL-12, IL-3, or GM-CSF in the presence of iDCs. Among these cytokines examined, only IL-15 showed an IL-2-like potential to provoke the production of IL-5 from the iNKT cells (Fig. 1*D*). Of note, receptors for IL-4, IL-7, IL-9, and IL-15 share γ-chain of IL-2R referred to as the common γ-chain, whereas IL-15R also shares β-chain with IL-2R. This implies that the intermediate affinity IL-2R complex composed of the β- and γ-chains would mediate signals needed for IL-5 production. Of further interest, an addition of exogenous IL-5 induced a low but significant amount of IL-4 production. This raises a possibility that, at least in some clones, IL-5 produced by iNKT cells in response to IL-2 may subsequently trigger IL-4 production from the same cells in an autocrine fashion or from other iNKT cells in the close vicinity, thereby augmenting the ability of iNKT cells to polarize the Th cell toward Th2.

Gene expression profile of iNKT cells responding to IL-2

To further confirm that our observations represent a previously overlooked property of iNKT cells, we conducted a comprehensive gene expression analysis. An Affymetrix DNA microarray was applied to characterize the mRNA expression of four IL-5-producing clones Kn.1, Kn.2, Kai.2, and Nkj.2. The results showed that 43 genes were significantly up-regulated following IL-2 stimulation in the presence of iDCs (Table II). Most notably, *IL5* was identified as the gene with the highest increase of expression after simulation (fold increase = 18.86). As the direct consequence of IL-2 stimulation, IL-2Rα (*IL2RA*) was ranked as the second (fold increase = 13.70) and IL-2Rγ (*IL2RG*) as the 40th (fold increase = 2.8). Furthermore, *IL13* was ranked as the third (fold increase = 11.4), whereas neither *IL4* nor *IFNG* was among the genes significantly up-regulated in the examined culture condition. The increased expression of *IL13* prompted us to measure the content of the encoded protein in the supernatant by using ELISA. Consistent with the microarray data, the IL-5-producing clones were found to secrete a large amount of IL-13 as well (Fig. 2). These results indicate that the selective production of IL-5 and IL-13 in response to IL-2 could be a significant property of a subset of $CD4^+$ iNKT cells.

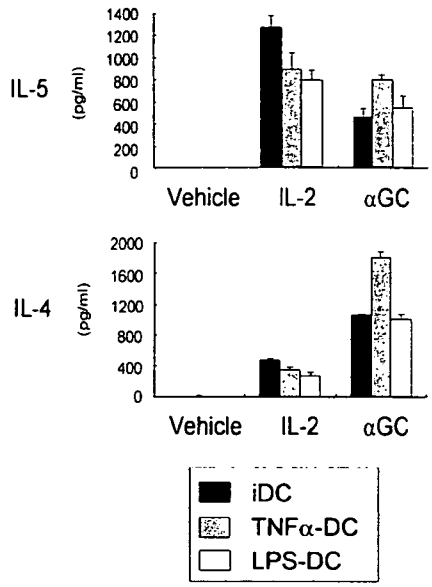

FIGURE 4. Comparison of the ability to induce IL-5 between iDC and mature DCs. The ability of iDCs and mature DCs to induce IL-5 from CD4+ iNKT cells in the presence of IL-2 was compared. To obtain mature DCs, iDCs were further stimulated with TNF-α (10 ng/ml) or LPS (2 ng/ml) for 12 h (designated as TNF-α-DC and LPS-DC, respectively). Representative IL-5 producing clones, Sk.1 and Oz, were stimulated with IL-2 (10 IU/ml) or αGC (100 ng/ml) using these DC populations. Similar results were obtained by both clones. Shown here is the representative data of Sk.1. Supernatants were collected after 48 h and IL-5/IL-4 production was measured by CBA.

Requirement of TCR-CD1d interaction for the selective IL-5 production by iNKT cells

We have further addressed whether the IL-5 production from the iNKT cell clones may be induced in the absence of iDCs. When we stimulated iNKT cells with exogenous IL-2 in the absence of iDCs, only a trace amount of IL-5 was detected (Fig. 3*A*), elucidating the requirement of iDCs. To determine whether iNKT cells would interact with iDCs via TCR or accessory molecules, we next cultured the iNKT cell clones with CD1d-transfected or mock-transfected HeLa cells and again examined the effect of IL-2. The results showed that CD1d-transfected cells could serve as efficient APCs for the IL-5 production induced by IL-2 (Fig. 3*B*), whereas mock-treated cells could not. To clarify whether IL-5 production after iNKT cell interaction with iDC also depends on CD1d, we examined the effect of the CD1d-blocking Ab (aCD1d59) on IL-5 production from the iNKT-iDC coculture. As shown in Fig. 3*C*, addition of the anti-CD1d Ab significantly reduced IL-5 production in response to IL-2. This indicates that TCR-CD1d interaction is critical for iNKT cell clones to produce IL-5, supporting the involvement of TCR signaling. Autoreactive iNKT cells are generally thought to recognize endogenous ligands loaded onto CD1d molecules. Therefore, we tried to stimulate iNKT cells with CD1d dimer (dimer X) loaded with iGb3, a recently identified endogenous ligand for iNKT cells (30, 31). However, loading iGb3 to dimer X was not successful in inducing IL-5 production. When cultured on a plastic plate precoated simply with unloaded dimer X, iNKT cells did not respond to IL-2 (data not shown). We also used TNF-α- or LPS-induced mature DCs as APCs for comparison with iDCs, assuming that up-regulated costimulatory molecules in mature DCs may help further promote IL-5 production (Fig. 4). Regarding αGC-induced IL-5 or IL-4 production, TNF-α-induced mature DCs appeared to be more potent than iDCs. In contrast,

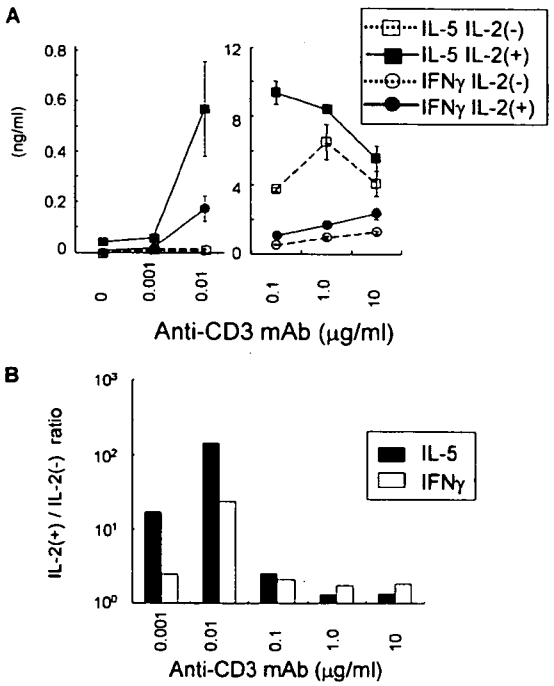

FIGURE 5. Suboptimal anti-CD3 stimulation mimics the effect of CD1d+ APCs for IL-5 induction from CD4+ iNKT clones in the presence of IL-2. CD4+ iNKT cell clones Kn.2 and Kai.2 were stimulated by plate-bound anti-CD3 mAb (0.001–10 μg/ml) in the presence or absence of IL-2 (10 IU/ml). IL-5 and IFN-γ in the supernatant were measured by using ELISA. Clones Kn.2 and Kai.2 gave similar results. Shown are representative data obtained from Kn.2. Data represent mean cytokine concentration from triplicate samples and error bars indicate +SD. *A*, Production of IL-5 and IFN-γ when stimulated with various concentrations of plate bound anti-CD3 Ab. Horizontal axis indicates concentration of anti-CD3 mAb used (micrograms per milliliter), whereas amount of the cytokines (nanograms per milliliter) are shown in vertical axis. *B*, The effect of exogenous IL-2 on the cytokine values. To evaluate the augmenting effect of exogenous IL-2 on cytokine production, the amounts of cytokine produced at the presence of IL-2 were divided by those obtained at the absence of IL-2. This IL-2+-IL-2− ratio was obtained using the data shown in *A*. Exogenous IL-2 induced IL-5 most efficiently and selectively when iNKT clones were stimulated at a suboptimal dose of anti-CD3 (0.01 μg/ml).

iDCs seemed as potent as mature DCs in the induction of IL-5 production by iNKT cells in response to IL-2, indicating that the IL-2-induced IL-5 response is not heavily influenced by the maturation state of DCs.

Suboptimal anti-CD3 stimulation with exogenous IL-2 promotes IL-5 production

As demonstrated above, CD1d expression on APCs (Fig. 3*B*) as well as the presence of exogenous IL-2 is critically required for IL-5 induction from iNKT cells. Our speculation is that IL-5-producing iNKT cells are autoreactive to CD1d ligand, but they cannot mount the detectable IL-5 response unless accessory IL-2 signaling is provided. This is based on the premise that the endogenous ligand expressed by DCs could not provide sufficiently strong TCR signals able to provoke IL-5 production. To test this hypothesis, we explored whether suboptimal cross-linking of TCR in the presence of IL-2 could induce selective IL-5 production. We stimulated iNKT cells with plate-bound anti-CD3 mAb in the presence of IL-2. Using this APC-free system, we found that even without adding IL-2, the iNKT clone cells produce a large amount of IL-5 and somewhat a lesser amount of IFN-γ at higher concentrations of anti-CD3 mAb (0.1, 1.0, and 10 μg/ml)

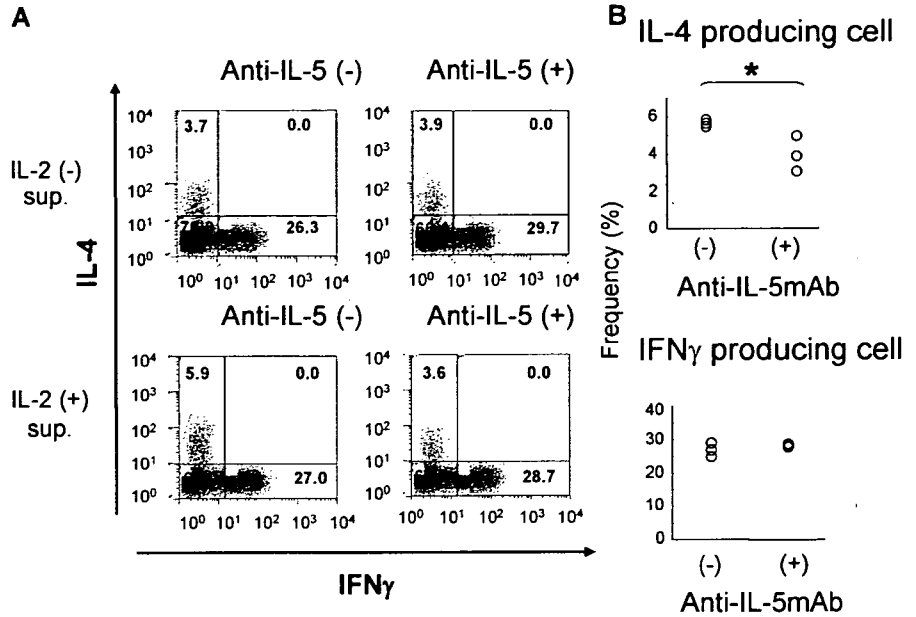

FIGURE 6. iNKT/iDC coculture supernatant induced Th2 CD4 T cell differentiation in an IL-5-dependent way. Here, we stimulated naive CD4 T cells with plate bound-anti-CD3 mAb (10 μg/ml) and soluble anti-CD28 mAb (2 μg/ml) and evaluated the effect of adding IL-2-induced IL-5-enriched supernatant from iNKT/iDC coculture (Kn.2). The presence of IL-5 in IL-2^+ sup and its absence in IL-2^- sup was confirmed by CBA before the assay. To evaluate the effect of IL-5 in the iNKT/iDC supernatant, assays were also conducted in the presence of anti-IL-5-neutralizing mAb. Seven days after culture, cells were harvested and intracellular cytokines (IL-4 and IFN-γ) were stained after 6 h PMA/ionomycin stimulation. *A*, Flow cytometry analysis of intracellular IL-4/IFN-γ staining of $CD4^+$ T cells following CD3/CD28 stimulation. The numbers indicate the percentage of cells in the given quadrant. More IL-4-producing cells were generated in the presence of IL-2^+ sup compared with IL-2^- sup. The number of IL-4-producing T cell was reduced when anti-IL-5 mAb was given. In contrast, the number of IFN-γ-producing cells remained unaffected. Shown here is a representative data of two separate experiments with consistent results. *B*, Effect of anti-IL-5 mAb on the induction of IL-4^+ or IFN-γ^+ T cells. The frequency of IL-4- or IFN-γ-producing cells after culture with IL-2^+ sup was determined as in *A*. In the presence of anti-IL-5 mAb, IL-4-producing cells were significantly reduced (the mean frequency dropped to 4.3% from 5.76%) (*, $p < 0.05$, one-factor ANOVA), whereas the frequency IFN-γ-producing cells stayed the same (the mean frequency was 27.0% and 28.2%).

(Fig. 5*A*). In this range of high Ab concentration, production of both IL-5 and IFN-γ was almost equally augmented by adding exogenous IL-2 (Fig. 5*B*), as judged by IL-2^+-IL-2^- ratios. As expected, the lower concentration of anti-CD3 (0.001 and 0.01 μg/ml) without IL-2 induced only trace amounts of IL-5 or IFN-γ from iNKT cell clones. However, when exogenous IL-2 was added, the production of the cytokines was greatly augmented (Fig. 5*A*). In particular, IL-5 production at 0.01 μg/ml anti-CD3 was greatly and selectively induced. The IL-2^+-IL-2^- ratio for IL-5 was 140.2, whereas that for IFN-γ was ~23.0 (Fig. 5*B*). As such, a suboptimal TCR stimulation with anti-CD3 could mimic the stimulation with $CD1d^+$ APCs, supporting our hypothesis that the suboptimal TCR and IL-2 signaling would cause IL-5 production from autoreactive iNKT cells.

IL-5 from iNKT cells promotes Th2 differentiation of naive $CD4^+$ T cells

Given that some $CD4^+$ iNKT cells selectively produce IL-5, it is important to know whether the iNKT cells may actively modulate an immune response by producing IL-5. To clarify this point further, we have collected the supernatant from iNKT cells that were stimulated with $CD1d^+$ iDCs and IL-2 (IL-2^+ sup), or from those stimulated with the iDCs alone (IL-2^- sup). Then, we examined the effect of adding these supernatants on in vitro differentiation of naive T cells induced with plate-bound anti-CD3 mAb stimulation. After 7 days of culture with the supernatant, the percentage of IL-4- or IFN-γ-producing $CD4^+$ T cells was enumerated by intracellular cytokine staining. The results showed that the addition of IL-2^+ sup induced higher frequencies of IL-4^+CD4^+ T cells, as compared with IL-2^- sup (5.9 vs 3.7% in Fig. 6*A*, *left*). In contrast, IFN-γ^+CD4^+ T cells did not differ significantly (27.0 vs 26.3%). Similar results were obtained in repeated experiments, indicating that IL-2^+ sup possess the biological activity to induce significant Th2 polarization of Th cells. To assess the role of IL-5 in the supernatant, we added neutralizing IL-5 Ab to the IL-2^+ sup and then evaluated its effect in the same culture system. The results showed that presence of anti-IL-5 significantly lowered the frequency of the IL-4^+CD4^+ T cells on day 7 (Fig. 6*B*, *upper*), whereas it did not change the percentage of IFN-γ^+ T cells (Fig. 6*B*, *upper*). Collectively, these results suggest that the IL-5 secreted by iNKT cells could contribute to mediating Th2 bias, although other factors such as IL-13 may also play some role.

Th2 cytokine deviation by IL-2 in BALB/c iNKT cells

The present results demonstrate that predominant production of IL-5, which has not been appreciated as an important property of iNKT cells, would characterize a proportion of autoreactive iNKT cell clones. Interestingly, the IL-5 response could be elicited by a weak TCR stimulus together with IL-2 or IL-15, which might occur during in vivo inflammatory reactions. However, one could argue that we might have seen an artifact arising from use of the iNKT cell clones that were repeatedly stimulated and expanded in vitro. To challenge this criticism, we examined the responsiveness of freshly separated mouse iNKT cells to $CD1d^+$ iDCs in the presence of IL-2. At the beginning, we tried to reproduce the results by using fresh human iNKT cells, but the low frequency of iNKT cells (0.01–0.1% of the PBMC) precluded our attempt. Therefore, freshly isolated iNKT cells and $CD11c^+$ DCs from

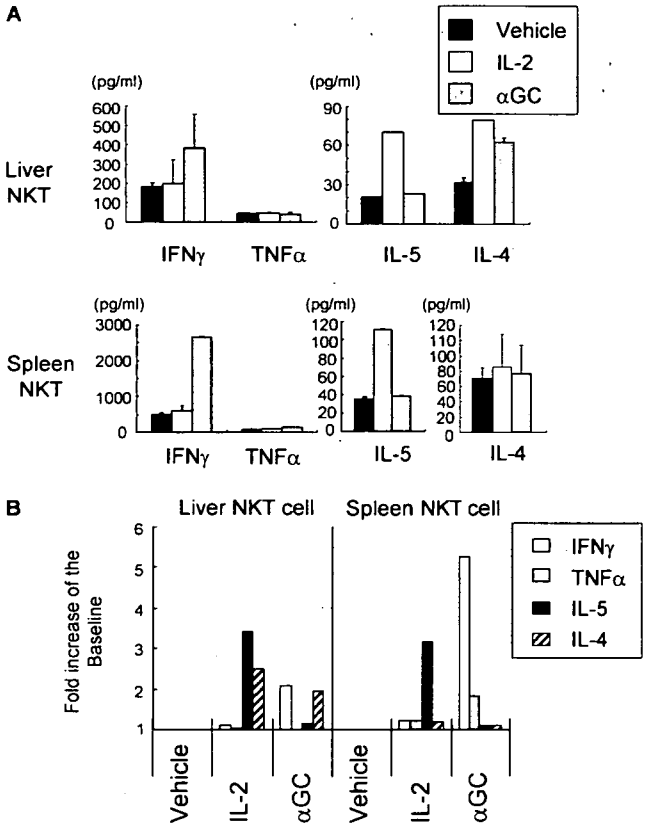

FIGURE 7. Freshly isolated iNKT cells from BALB/c mice produced IL-5 in the presence of IL-2. iNKT cells were isolated from livers and spleens pooled from six BALB/c mice of the same age by using αGC loaded-CD1d dimer X. iNKT cells were cocultured with magnetically isolated $CD11c^+$ splenocytes and stimulated with IL-2 or αGC for 72 h. Cytokines in the supernatant were evaluated by CBA. Data represent mean cytokine concentration from triplicate samples with error bars indicating +SD. Shown here is the representative data from three separate experiments, which gave similar results. *A*, Cytokine values (picograms per milliliter). *B*, Cytokine induction evaluated by fold increase from the baseline.

BALB/c mice were cocultured in the presence of IL-2 or αGC. Compared with human iNKT clone-iDC cocultures, the mouse cocultures showed a relatively high background response in any cytokine measured. However, as seen in humans, exogenous IL-2 apparently augmented the production of IL-5 from liver and spleen iNKT cells (Fig. 7), whereas neither IFN-γ nor TNF-α was altered by IL-2 stimulation. In contrast to IL-2, αGC stimulation induced a massive production of IFN-γ from liver and spleen iNKT cells and some TNF-α from spleen iNKT cells. However, IL-5 triggered by αGC was negligible.

To further convince ourselves of the significance of the physiological effect of IL-2 on iNKT cells, we investigated the effect of IL-2 on iNKT cells in vivo. We injected the cytokine i.v. to BALB/c mice. Two hours later, we separated liver lymphocytes and analyzed the intracellular expression of IL-5 by flow cytometry analysis. Consistent with the ex vivo IL-2 stimulation data, a significant increase in the number of IL-5-producing iNKT cells was observed in the BALB/c mice injected with IL-2, while a similar increase in the number of IFN-γ-producing iNKT cells could not be found (Fig. 8). These data imply that rodent iNKT cells are able to produce IL-5 ex vivo as well as in vivo in response to IL-2 as demonstrated in human iNKT clones. Taken together, we propose that this selective IL-5 production could represent a physiological iNKT cell response.

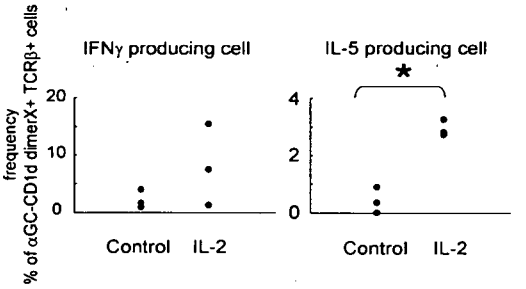

FIGURE 8. Increase of IL-5-producing iNKT cell by in vivo administration of IL-2. Liver lymphocyte were isolated after i.v. IL-2 administration and stained for intracellular IL-5 or IFN-γ production. The frequency of αGC-loaded CD1d dimer X^+ $TCR\beta^+$ iNKT cells was plotted for IL-5- and IFN-γ-producing cells. Each dot represents data obtained from one mouse. Three mice were used for each condition. IL-5-producing iNKT cells were significantly increased in IL-2 i.v. mice ($p < 0.05$, Welch's t test) though no significant difference was observed in IFN-γ-producing iNKT cells.

Discussion

The cardinal property of iNKT cells to produce regulatory cytokines has been well-documented in prior studies. It is, however, of note that the reagents used for inducing cytokines were either αGC, an unnatural ligand for iNKT cells, or anti-CD3 Ab in most cases. These reagents would transmit potent TCR signaling, thereby provoking production of a very wide range of Th1 and Th2 cytokines from iNKT cells. Therefore, it is still unclear as to which cytokines are naturally secreted and which are not involved in physiological immune regulation during the natural course of diseases. In this study, we have reported that some human $CD4^+$ iNKT cell clones could selectively produce enormous amounts of IL-5 and IL-13 when cultured with $CD1d^+$ APCs in the presence of IL-2 or IL-15. Importantly, the amount of IL-5 was even higher than that induced by αGC. Moreover, DNA microarray analysis identified *IL5* and *IL13* as the genes that were most highly upregulated during their response to $CD1d^+$ APCs in the presence of IL-2. Subsequent analysis showed that plate-bound anti-CD3 Ab could replace the $CD1d^+$ APCs, suggesting that iNKT cells may exhibit the IL-5-producing function after recognizing an endogenous self-ligand expressed by APCs. Also, the IL-5-enriched supernatant from the iNKT cells showed a Th2-biasing effect in vitro, which could be blocked by neutralizing anti-IL-5 mAb. Finally, we showed that freshly isolated iNKT cells could also produce IL-5 in response to $CD1d^+$ DCs in the presence of IL-2. These results indicate that a subset of $CD4^+$ iNKT cells may use IL-5 and IL-13 as important mediators to regulate Th cell responses in vivo. It is likely that the iNKT cells producing these cytokines may play a decisive role in the control of Th1-mediated pathogenesis or mediating allergic conditions.

It has been well-recognized freshly isolated iNKT cells express activation markers such as CD69 even shortly after birth (23, 35). Together with the recent discovery that iGb3 could serve as an endogenous ligand for iNKT cells (30, 31), it is generally accepted that iNKT cells are autoreactive cells that are being constantly stimulated by self-ligand(s). Consistent with this concept, studies have shown that a proportion of iNKT cell clones exhibit various degrees of self-reactivity as measured by proliferative responses against $CD1d^+$ APCs (29, 36). However, it has remained unclear what percentage of iNKT cells may exhibit such an autoreactive response as demonstrated by simple proliferation assays. In this regard, it is noteworthy that the self-reactivity of our iNKT cell clones could be demonstrated by using their ability to produce IL-5

in the presence of IL-2 as a readout. We assume that such a weak self-reactivity of the cells has hampered identifying this potentially important iNKT cell subset in prior studies.

Although we added rIL-2 and IL-15 exogenously to stimulate iNKT cells, these are the cytokines commonly produced in the inflammatory milieu. This allows us to speculate that the IL-5-producing iNKT cells might have a chance to encounter CD1d$^+$ APCs in the presence of either of the cytokines, thereby playing an important role in the local control of inflammation. Interestingly, IL-15 blockade has recently been shown to prevent the induction of allergic airway inflammation (37), implicating indirect evidence for the presence of IL-15 in the site of airway inflammation. Although this study has not identified iNKT cells as a target of IL-15, the critical role of iNKT cells shown in other rodent studies (14, 15) and human asthma (38) supports the idea that local IL-15 may stimulate iNKT cells to produce IL-5 and IL-13, which then leads to augmentation of allergic inflammation involving activation of eosinophils (39, 40). Another point of interest is that the role of IL-2 has been indicated in Th2 polarization processes involving iNKT cells. Although this is most elegantly shown in the case of eradication of certain parasites (41, 42), it is possible that iNKT cells are the target of IL-2 for inducing Th2 polarization. It is also likely that iNKT cells in the inflammatory lesions of MS may produce IL-5 or IL-13 after being triggered by IL-2 or IL-15 in the inflammatory lesions. The IL-5 produced by iNKT cells may directly promote Th2 cell differentiation, thereby deviating Th1/Th2 balance toward Th2. Alternatively, Th2 polarization could be mediated by other cytokines that were triggered by IL-5 in an autocrine or paracrine fashion. In fact, we showed that IL-4 was induced by the IL-5-producing iNKT cells in the presence of IL-5 (Fig. 1*D*) and overproduction of IL-4 from CD4$^+$ iNKT cells could be demonstrated in the remission state of MS (33).

Recent reports have shown that striking Th1 responses against exogenous pathogens could be triggered by iNKT cells after recognizing an endogenous ligand in the presence of IL-12 (26, 31). Given its remarkable homology to the IL-5 response triggered by IL-2 reported here in this article, we speculate that stimulation with an endogenous ligand and locally produced cytokines is a fundamental mechanism that would lead iNKT cells to provoke a decisive response for dealing with infection, allergy, and autoimmunity. In infection models, iNKT cell recognition of iGb3 has been identified as an important trigger for inducing Th1 response by iNKT cells (31). However, iNKT cells may recognize different endogenous Ags (43) and therefore the microenvironment of different tissues or types of inflammation (e.g., Th1 vs Th2) encountered may be instrumental in determining the phenotype of iNKT cytokine production. In this regard, endogenous ligand(s) involved in IL-5 production by IL-2 is an area to be further investigated in the future.

It is important to realize that as much as 8 of the 26 CD4$^+$ iNKT clones (Table I) have demonstrated a bias for IL-5 production following IL-2 stimulation. We speculate that this could arise from the heterogeneity of β-chain CDR3 sequence, although this point is another area that needs to be formally verified. Supportive of this speculation is the recent study showing that individual TCR β-chain may contribute to the variation of Ag recognition among iNKT cells (36). Another possibility is that these IL-5-producing iNKT cells may comprise a distinct lineage with the unique machinery to overproduce IL-5. It may also be due to differences in the frequency of IL-5-biased iNKT cells among each individual. This idea is supported by the observation that IL-5-biased clones tended to be generated from the same individuals (Table I). Furthermore, our preliminary data has demonstrated that IL-2-dependent production from iNKT cells might be subject to mouse strain differences: namely, the production of IL-5 from iNKT cells found in BALB/c could not be demonstrated in C57BL/6 mice (data not shown). This discrepancy between Th1 (C57BL/6) and Th2 (BALB/c) polarized mice may give us an important clue to further analyze this issue.

In summary, the present study has identified presence of human CD4$^+$ iNKT cells that produce IL-5 and IL-13 in response to suboptimal TCR stimulation together with IL-2 or IL-15. Previous studies using αGC or anti-CD3 Ab for stimulation of iNKT cells was unsuccessful in revealing the identity and the unique property of these iNKT cells, reflecting the nonphysiological nature of the methods used for stimulating iNKT cells. Analysis of our data and studies from other groups suggest that this iNKT cell population produce IL-5 and IL-13 in vivo by recognizing an endogenous ligand. In the pathogenesis of allergy, autoimmune diseases or parasite infection, CD4$^+$ iNKT may play a key role in deviating immune responses toward Th2 and thus provide a suitable target for immune intervention. Our results also imply that cytokines could play a major role in instructing the iNKT cell populations to respond differentially in vivo, whether it is beneficial or hazardous. Taking all these into consideration, we propose that sensing the presence of cytokines is probably one of the most fundamental abilities for the iNKT cells that are to be given only a weak TCR signal in vivo.

Acknowledgments

We thank Dr. J. Ludovic Croxford for helpful comments, Yuki Kikai for cell sorting, and Hiromi Yamaguchi for cell culture.

Disclosures

The authors have no financial conflict of interest.

References

1. Bendelac, A., M. Bonneville, and J. F. Kearney. 2001. Autoreactivity by design: innate B and T lymphocytes. *Nat. Rev. Immunol.* 1: 177–186.
2. Taniguchi, M., M. Harada, S. Kojo, T. Nakayama, and H. Wakao. 2003. The regulatory role of Vα14 NKT cells in innate and acquired immune response. *Annu. Rev. Immunol.* 21: 483–513.
3. Wilson, B. S., and T. L. Delovitch. 2003. Janus-like role of regulatory iNKT cells in autoimmune disease and tumour immunity. *Nat. Rev. Immunol.* 3: 211–222.
4. Kronenberg, M. 2005. Toward an understanding of NKT cell biology: progress and paradoxes. *Annu. Rev. Immunol.* 23: 877–900.
5. Kawano, T., J. Cui, Y. Koezuka, Y. Toura, Y. Kaneko, K. Motoki, H. Ueno, R. Nakagawa, H. Sato, E. Kondo, et al. 1997. CD1d-restricted and TCR-mediated activation of Vα14 NKT cells by glycosylceramides. *Science* 278: 1626–1629.
6. Godfrey, D. I., H. R. MacDonald, M. Kronenberg, M. J. Smyth, and L. van Kaer. 2004. NKT cells: what's in a name? *Nat. Rev. Immunol.* 4: 231–237.
7. Duarte, N., M. Stenstrom, S. Campino, M. L. Bergman, M. Lundholm, D. Holmberg, and S. L. Cardell. 2004. Prevention of diabetes in nonobese diabetic mice mediated by CD1d-restricted nonclassical NKT cells. *J. Immunol.* 173: 3112–3118.
8. Terabe, M., J. Swann, E. Ambrosino, P. Sinha, S. Takaku, Y. Hayakawa, D. I. Godfrey, S. Ostrand-Rosenberg, M. J. Smyth, and J. A. Berzofsky. 2005. A nonclassical non-Vα14-Jα18 CD1d-restricted (type II) NKT cell is sufficient for down-regulation of tumor immunosurveillance. *J. Exp. Med.* 202: 1627–1633.
9. Gumperz, J. E., S. Miyake, T. Yamamura, and M. B. Brenner. 2002. Functionally distinct subsets of CD1d-restricted natural killer T cells revealed by CD1d tetramer staining. *J. Exp. Med.* 195: 625–636.
10. Lee, P. T., K. Benlagha, L. Teyton, and A. Bendelac. 2002. Distinct functional lineages of human Vα24 natural killer T cells. *J. Exp. Med.* 195: 637–641.
11. Kim, H. Y., H. J. Kim, H. S. Min, S. Kim, W. S. Park, S. H. Park, and D. H. Chung. 2005. NKT cells promote antibody-induced joint inflammation by suppressing transforming growth factor β1 production. *J. Exp. Med.* 201: 41–47.
12. Chiba, A., S. Kaieda, S. Oki, T. Yamamura, S. Miyake, and 2005. The involvement of Vα14 NKT cells in the pathogenesis of arthritis in murine models. *Arthritis Rheum.* 52: 1941–1948.
13. Ohnishi, Y., A. Tsutsumi, D. Goto, S. Itoh, I. Matsumoto, M. Taniguchi, and T. Sumida. 2005. TCR Vα14 natural killer T cells function as effector T cells in mice with collagen-induced arthritis. *Clin. Exp. Immunol.* 141: 47–53.
14. Akbari, O., P. Stock, E. Meyer, M. Kronenberg, S. Sidobre, T. Nakayama, M. Taniguchi, M. J. Grusby, R. H. DeKruyff, and D. T. Umetsu. 2003. Essential role of NKT cells producing IL-4 and IL-13 in the development of allergen-induced airway hyperreactivity. *Nat. Med.* 9: 582–588.
15. Lisbonne, M., S. Diem, A. de Castro Keller, J. Lefort, L. M. Araujo, P. Hachem, J.-M. Fourneau, S. Sidobre, M. Kronenberg, M. Taniguchi, et al. 2003. Cutting

edge: invariant Vα14 NKT cells are required for allergen-induced airway inflammation and hyperreactivity in an experimental asthma model. *J. Immunol.* 171: 1637–1641.
16. Godfrey, D. I., and M. Kronenberg. 2004. Going both ways: immune regulation via CD1d-dependent NKT cells. *J. Clin. Invest.* 114: 1379–1388.
17. Chen, H., and W. E. Paul. 1997. Cultured NK1.1$^+$CD4$^+$ T cells produce large amounts of IL-4 and IFN-γ upon activation by anti-CD3 or CD1. *J. Immunol.* 159: 2240–2249.
18. Schmieg, J., G. Yang, R. W. Franck, and M. Tsuji. 2003. Superior protection against malaria and melanoma metastases by a c-glycoside analogue of the natural killer T cell ligand α-galactosylceramide. *J. Exp. Med.* 198: 1631–1641.
19. Miyamoto, K., S. Miyake, and T. Yamamura. 2001. A synthetic glycolipid prevents autoimmune encephalomyelitis by inducing Th2 bias of natural killer T cells. *Nature* 413: 531–534.
20. Miyake, S., and T. Yamamura. 2005. Therapeutic potential of glycolipid ligands for natural killer (NK) T cells in the suppression of autoimmune disease. *Curr. Drug Targets Immune Endocr. Metabol. Disord.* 5: 315–322.
21. Heller, F., I. J. Fuss, E. E. Nieuenhuis, R. S. Blumberg, and W. Strober. 2002. Oxazolone colitis, a Th2 colitis model resembling ulcerative colitis, is mediated by IL-13-producing NK-T cells. *Immunity* 17: 629–638.
22. D'Andrea, A., D. Goux, C. De Lalla, Y. Koezuka, D. Montagna, A. Moretta, P. Dellabona, G. Casorati, and S. Abrignani. 2000. Neonatal invariant Vα24$^+$ NKT lymphocytes are activated memory cells. *Eur. J. Immunol.* 30: 1544–1550.
23. Park, S. H., K. Benlagha, D. Lee, E. Balish, and A. Bendelac. 2000. Unaltered phenotype of, tissue distribution and function of Vα14$^+$ NKT cells in germ-free mice. *Eur. J. Immunol.* 30: 620–625.
24. Matsuda, J. L., L. Gapin, J. L. Baron, S. Sidobre, D. B. Stetson, M. Mohrs, R. M. Locksley, and M. Kronenberg. 2003. Mouse Vα14i natural killer T cells are resistant to cytokine polarization in vivo. *Proc. Natl. Acad. Sci. USA* 100: 8395–8400.
25. Oki, S., A. Chiba, T. Yamamura, and S. Miyake. 2004. The clinical implication and molecular mechanism of preferential IL-4 production by modified glycolipid-stimulated NKT cells. *J. Clin. Invest.* 113: 1631–1640.
26. Brigl, M., L. Bry, S. C. Kent, J. E. Gumperz, and M. B. Brenner. 2003. Mechanism of CD1d-restricted natural killer T cell activation during microbial infection. *Nat. Immunol.* 4: 1230–1236.
27. Joyce, S., A. S. Woods, J. W. Yewdell, J. R. Bennink, D. De Silva, A. Boesteanu, S. P. Balk, R. J. Cotter, and R. R. Brutkiewicz. 1998. Natural ligand of mouse CD1d1; cellular glycosylphosphatidylinositol. *Science* 279: 1541–1544.
28. Gumperz, J. E., C. Roy, A. Makowska, D. Lum, M. Sugita, T. Podrebarac, Y. Koezuka, S. Porceli, S. Cardell, M. B. Brenner, and S. M. Behar. 2000. Murine CD1d-restricted T cell recognition of cellular lipids. *Immunity* 12: 211–221.
29. Rauch, J., J. E. Gumperz, C. Robinson, M. Skold, C. Roy, D. C. Young, M. Lafler, B. D. Moody, M. B. Brenner, and C. E. Costello. 2003. Structural features of the acyl chain determine self-phospholipid antigen recognition by a CD1d-restricted invariant NKT (iNKT) cell. *J. Biol. Chem.* 278: 47508–47515.
30. Zhou, D., J. Mattner, C. Cantu, 3rd, N. Schrantz, N. Yin, Y. Gao, Y. Sagiv, K. Hudspeth, Y. Wu, T. Yamashita, et al. 2004. Lysosomal glycosphingolipid recognition by NKT cells. *Science* 306: 1786–1789.
31. Mattner, J., K. L. Debord, N. Ismail, R. D. Goff, C. Cantu, 3rd, D. Zhou, P. Saint-Mezard, V. Wang, Y. Gao, N. Yin, et al. 2005. Exogenous and endogenous glycolipid antigens activate NKT cells during microbial infections. *Nature* 434: 525–529.
32. Thomas, S. Y., R. Hou, J. E. Boyson, T. K. Means, C. Hess, D. P. Olson, J. L. Strominger, M. B. Brenner, J. E. Gumperz, S. B. Wilson, and A. D. Luster. 2003. CD1d-restricted NKT cells express a chemokine receptor profile indicative of Th1-type inflammatory homing cells. *J. Immunol.* 171: 2571–2580.
33. Araki, M., T. Kondo, J. E. Gumperz, M. B. Brenner, S. Miyake, and T. Yamamura. 2003. Th2 bias of CD4$^+$ NKT cells derived from multiple sclerosis in remission. *Int. Immunol.* 15: 279–288.
34. Takahashi, K., T. Aranami, M. Endoh, S. Miyake, and T. Yamamura. 2004. The regulatory role of natural killer cells in multiple sclerosis. *Brain* 127: 1917–1927.
35. van Der Vliet, H. J., N. Nishi, T. D. de Gruijl, B. M. von Blomberg, A. J. van den Eertwegh, H. M. Pinedo, G. Giaccone, and R. J. Scheper. 2000. Human natural killer T cells acquire a memory-active phenotype before birth. *Blood* 95: 2440–2442.
36. Brigl, M., P. van den Elzen, X. Chen, J. H. Meyers, D. Wu, C.-H. Wong, F. Reddington, P. A. Illarianov, G. S. Besra, M. B. Brenner, and J. E. Gumperz. 2006. Conserved and heterogeneous lipid antigen specificities of CD1d-restricted NKT cell receptors. *J. Immunol.* 176: 3625–3634.
37. Ruckert, R., K. Brandt, A. Braun, H.-G. Hoymann, U. Herz, V. Budagian, H. Durkop, H. Renz, and S. Bulfone-Paus. 2005. Blocking IL-15 prevents the induction of allergen-specific T cells and allergic inflammation in vivo. *J. Immunol.* 174: 5507–5515.
38. Akbari, O., J. L. Falu, J. L. Hoyte, G. J. Berry, J. Wahlstrom, M. Kronenberg, R. H. DeKruyff, and D. T. Umetsu. 2006. CD4$^+$ invariant T-cell-receptor$^+$ natural killer T cells in bronchial asthma. *N. Engl. J. Med.* 354: 1117–1129.
39. Yamaguchi, Y., T. Suda, J. Suda, M. Eguchi, Y. Miura, N. Harada, A. Tominaga, and K. Takatsu. 1988. Purified interleukin 5 supports the terminal differentiation and proliferation of murine eosinophilic precursors. *J. Exp. Med.* 167: 43–56.
40. Yamaguchi, Y., Y. Hayashi, Y. Sugama, Y. Miura, T. Kasahara, S. Kitamura, M. Torisu, S. Mita, A. Tominaga, and K. Takatsu. 1988. Highly purified murine interleukin (IL-5) stimulates eosinophil function and prolongs in vitro survival: IL-5 as eosinophil chemotactic factor. *J. Exp. Med.* 167: 1737–1742.
41. Cui, J., N. Watanabe, T. Kawano, M. Yamashita, T. Kamata, C. Shimizu, M. Kimura, E. Shimizu, J. Koike, H. Koseki, et al 1999. Inhibition of T helper cell type 2 cell differentiation and immunoglobulin E response by ligand-activated Vα14 natural killer T cells. *J. Exp. Med.* 190: 783–792.
42. Mallevaey, T., J. P. Zanetta, C. Faveeuw, J. Fontain, E. Maes, F. Platt, M. Capron, M. L. de-Moraes, and F. Trottein. 2006. Activation of invariant NKT cells by the helminth parasite *Schistosoma mansoni*. *J. Immunol.* 176: 2476–2485.
43. Porubsky, S., A. O. Speak, B. Luckow, V. Cerundolo, F. M. Platt, and H.-J. Grone. 2007. Normal development and function of invariant natural killer T cells in mice with isoglobosylceramide (iGb3) deficiency. *Proc. Natl. Acad. Sci. USA* 104: 5977–5982.

ARTHRITIS & RHEUMATISM
Vol. 56, No. 6, June 2007, pp 2018–2030
DOI 10.1002/art.22645

Comprehensive Investigation of Disease-Specific Short Peptides in Sera From Patients With Systemic Sclerosis

Complement C3f-des-arginine, Detected Predominantly in Systemic Sclerosis Sera, Enhances Proliferation of Vascular Endothelial Cells

Yang Xiang,[1] Toshihiro Matsui,[2] Kosuke Matsuo,[3] Kota Shimada,[2] Shigeto Tohma,[2] Hiroshi Nakamura,[3] Kayo Masuko,[3] Kazuo Yudoh,[3] Kusuki Nishioka,[3] and Tomohiro Kato[3]

Objective. **To identify pathogenic and/or disease-specific short peptides in sera from patients with systemic sclerosis (SSc).**

Methods. **Serum samples from 40 patients with SSc, 30 patients with systemic lupus erythematosus, 21 patients with rheumatoid arthritis, 30 patients with osteoarthritis, and 26 healthy donors were tested. Short peptides with molecular weights of smaller than ~3 kd, purified from the sera by magnetic bead–based hydrophobic interaction chromatography 18, were detected and their amino acid sequences determined using matrix-assisted laser desorption ionization–time-of-flight mass spectrometry. Effects of the identified peptides on fibroblasts and microvascular endothelial cells were tested using synthesized peptides and sera containing the peptides.**

Results. **A group of peptides with mass/charge (m/z) values of 1,865, 1,778, 1,691, 1,563, and 1,450 were detected predominantly in the SSc sera. These peptides were identified as family members of complement C3f-des-arginine (DRC3f) derived from C3b. The level of DRC3f (m/z 1,865) was related to vascular involvement in SSc and to SSc disease activity. The synthesized peptides of DRC3f and C3f, as well as the filtrated sera containing DRC3f, enhanced proliferation of microvascular endothelial cells, but not fibroblasts. Both DRC3f and C3f increased production of transforming growth factor β1 by dermal microvascular endothelial cells.**

Conclusion. **This comprehensive peptidomics analysis revealed the predominance of DRC3f in the sera of patients with SSc. Investigation of DRC3f may be a useful tool for the diagnosis and evaluation of disease activity in SSc. Moreover, its demonstrated effects on endothelial cells suggest a potential role for DRC3f in the pathophysiologic mechanisms of SSc.**

Systemic sclerosis (SSc) is an autoimmune disorder of the connective tissue, characterized by widespread vascular lesions and fibrosis. Raynaud's phenomenon, increased thickness of the vascular wall, devascularization, and thickness of the basement membrane are typical features of SSc. The digital arteries of patients with SSc exhibit marked intimal proliferation, resulting in severe narrowing and occlusion of arterial lumen and limited vasodilative responses to vasodilator therapies (1).

Thus far, the contributions of many molecules to the pathogenesis and diagnosis of SSc have been reported (2–9). Investigation of these known molecules is of great value for the understanding of SSc pathogenesis; however, it would also be important to identify novel SSc-related molecules by hypothesis-free comprehensive

Supported in part by a grant-in-aid from the Japanese Ministry of Health, Labor, and Welfare, by the Japanese Ministry of Education, Culture, Sports, Science, and Technology, and by the Japan Rheumatism Association.

[1]Yang Xiang, MD, PhD: St. Marianna University School of Medicine, Kawasaki, Kanagawa, Japan, and University Hospital, Hubei University for Nationalities, Enshi, Hubei, China; [2]Toshihiro Matsui, MD, PhD, Kota Shimada, MD, Shigeto Tohma, MD: Sagamihara National Hospital, Sagamihara, Kanagawa, Japan; [3]Kosuke Matsuo, MD, PhD, Hiroshi Nakamura, MD, PhD, Kayo Masuko, MD, PhD, Kazuo Yudoh, MD, PhD, Kusuki Nishioka, MD, Tomohiro Kato, MD, PhD: St. Marianna University School of Medicine, Kawasaki, Kanagawa, Japan.

Address correspondence and reprint requests to Tomohiro Kato, MD, PhD, Director, Department of Bioregulation and Proteomics, Institute of Medical Science, St. Marianna University School of Medicine, 2-16-1 Sugao, Miyamae-ku, Kawasaki, Kanagawa 216-8512, Japan. E-mail: t3kato@marianna-u.ac.jp.

Submitted for publication June 5, 2006; accepted in revised form February 16, 2007.

surveillance. In this regard, genomic surveillance using single-nucleotide polymorphisms, DNA arrays for messenger RNA expression, and proteomic surveillance have been used recently (10). These techniques can detect various molecules that may be involved in the pathogenesis of SSc or that may be useful for diagnosis. However, the targets of surveillance have been limited to genes or relatively large proteins. Peptides with low molecular weights (smaller than ~3 kd) generally cannot be investigated by these techniques.

Peptides with such low molecular weights often play a central role in biologic and pathologic processes. Typical of these peptides would be bradykinin, which is a peptide that is only 9 amino acid residues in length and produced from kininogen by specific proteolysis. Another example would be substance P, in a neuropeptide of 11 amino acid residues. Peptides with such low molecular weights are estimated to be produced in large amounts by proteolysis of large proteins, which thereby generates various bioactive and/or diagnostically useful short peptides in addition to the known peptides in the body. However, there are only a few ways to survey such peptides efficiently. Quite recently, mass spectrometry methods that directly detect and identify peptides with low molecular weights and with low concentrations (referred to as peptidomics analysis) have been developed. This offers a promising approach to the discovery of novel short peptides that could be useful in the diagnosis and treatment of diseases (11–13).

In the present study, we aimed to identify low molecular weight peptides in the serum of patients with SSc in order to understand the role of these peptides in disease pathogenesis, which could lead to better diagnosis and treatment of SSc. By combining a microamount peptide-separating method with magnetic beads and matrix-assisted laser desorption ionization–time-of-flight (MALDI-TOF) mass spectrometry, we were able to comprehensively detect short peptides in the sera of patients with SSc, those with non-SSc rheumatic diseases, and healthy donors. In comparing the results between each group of samples, we found that the sera of patients with SSc carried complement C3f-des-arginine (DRC3f) and its degraded smaller fragments at very high levels and with high frequency, compared with the sera of patients with non-SSc rheumatic diseases or healthy donors. Furthermore, we demonstrated that these peptides promoted proliferation of human microvascular endothelial cells (HMVECs) in vitro. The results of this study will open a new field of investigation into the pathophysiologic processes of SSc.

PATIENTS AND METHODS

Patients. Forty patients with SSc (1 man and 39 women) whose diagnosis fulfilled the American College of Rheumatology (ACR; formerly, the American Rheumatism Association) criteria for SSc (14) were studied. The mean age of these SSc patients was 56.4 years (range 29–83 years). The duration of SSc was defined as the period from the date of onset of the disease to the date of blood sampling. Appearance of the first SSc symptom was defined as the first presentation of a symptom, even if it was before the date of diagnosis. The mean disease duration among the patients with SSc was 6.83 years (range 3–441 months). Skin changes were recorded using the modified Rodnan total skin thickness score (15).

Twenty-six serum samples from age- and sex-matched healthy donors (1 man and 25 women) were selected as controls for the SSc samples. The mean age of the control group was 55.6 years (range 27–84 years). In addition, 30 patients (3 men and 27 women) with systemic lupus erythematosus (SLE) (16) were enrolled. The mean age of the SLE patients was 47.2 years (range 23–83 years), and the mean SLE Disease Activity Index (SLEDAI) score (scale 0–105) (17) in these patients was 13.4 (range 7–28). Twenty-one patients with rheumatoid arthritis (RA) (2 men and 19 women) were also enrolled. The mean age of the RA patients was 60.1 years (range 36–78 years). Ten of the RA patients had an erythrocyte sedimentation rate (ESR) of higher than 30 mm/hour, and 18 RA patients had an elevated C-reactive protein (CRP) level. Finally, 30 patients (6 men and 24 women) with osteoarthritis (OA) were also enrolled in this study. The mean age of the OA patients was 64.4 years (range 46–84 years), and these patients were diagnosed according to the ACR criteria for knee OA (18).

The serum samples were stored at −80°C until used. All samples were obtained after subjects provided their informed consent, and the study was approved by the local institutional ethics committee.

Separation and purification of serum peptides. Serum peptides were separated and purified with a purification kit of magnetic beads, using magnetic bead–based hydrophobic interaction chromatography 18 (MB-HIC18) (Bruker Daltonics, Ettlingen, Germany) according to the manufacturer's instructions (19). Briefly, 5 μl of magnetic beads was mixed with 10 μl of MB-HIC18 binding solution and 5 μl of each serum sample, and the beads were then collected by a magnetic beads separator. After washing 4 times in an MB-HIC18 wash solution, we eluted the bound peptides off the beads into 5 μl of 50% acetonitrile, and then diluted 1 μl of the eluted peptide solution in 10 μl of matrix solution (0.3 mg/ml α-cyano-4-hydroxycinnamic acid in ethanol:acetone 2:1). Finally, 1 μl of the diluted eluate was loaded onto 600-μm–diameter spots on a metal plate for mass spectrometry analysis (AnchorChip; Bruker Daltonics).

Serum samples from the patients as well as from the healthy controls were filtered using 3.0-kd filters (Microcon; Millipore, Bedford, MA) at 15,000 revolutions per minute for 2 hours. Peptides in the flow-through fraction were concentrated with Ziptip-C18 (Millipore) and then eluted off the tip in 1 μl of 50% acetonitrile. The eluate was diluted in 10 μl of matrix solution, and 1 μl of the eluate–matrix mixture was then loaded on the AnchorChip target plate.

Mass spectrometry, identification of peptide sequences, and comparison of peptide profiles. The eluted peptides were detected with a MALDI-TOF mass spectrometer (Ultraflex; Bruker Daltonics). The mass spectra of the peptide peaks were initially detected in the automatic linear positive mode, for simple comparison between sample groups. Mass spectrometry analysis was then performed using the reflector mode, to obtain accurate masses of the peptides. Finally, MALDI-TOF analysis and a subsequent sequence search using the search engine Mascot (www.matrixscience.com) were performed to identify the sequences of the peptides of interest.

A comparative analysis of the mass spectra of the peptide peaks between SSc patients and healthy controls as well as between SSc patients and patients with other rheumatic diseases was performed using ClinPro Tools (CPT) software, version 1.0 (Bruker Daltonics) as previously described (19). To evaluate the relative levels of peptides in each serum sample, we defined the upper limit of normal range as the mean peak intensity + 3 SD of healthy control sera. Peptide levels in the serum from each patient, expressed in arbitrary units, were calculated according to the formula: arbitrary units = individual peak intensity/(mean peak intensity of healthy controls + 3 SD) × 100. The cutoff point to define a relative fold increase in peptide levels was set at 100 arbitrary units.

Preparation of peptides. The peptides of complement C3f, whose sequence is NH2-Ser-Ser-Lys-Ile-Thr-His-Arg-Ile-His-Trp-Glu-Ser-Ala-Ser-Leu-Leu-Arg-COOH (17 amino acid residues with peptide mass of 2,021 daltons), and DRC3f, whose sequence is NH2-Ser-Ser-Lys-Ile-Thr-His-Arg-Ile-His-Trp-Glu-Ser-Ala-Ser-Leu-Leu-COOH (16 amino acid residues with peptide mass of 1,865 daltons), were synthesized by solid-phase peptide synthesis and purified by RP-18 high-performance liquid chromatography as previously described (20). Fibrinopeptide A (FPA), purchased from Bachem (Bubendorf, Switzerland), was used as a control peptide.

Cell culture. Lung HMVECs and adult dermal HMVECs (both from Cell Systems, Kirkland, WA) were cultured in CS-C serum-free complete medium with a growth factor (SF-4Z0-500; Cell Systems) on type I collagen–coated Cellware plates (Becton Dickinson, Bedford, UK). Normal human dermal fibroblasts (Cambrex, Long Beach, CA) were cultured in RPMI 1640 medium (Sigma-Aldrich, Poole, UK) containing 10% fetal bovine serum (FBS) on tissue culture plates (Becton Dickinson). All cells were cultured at 37°C in a humidified atmosphere of 5% CO_2. The medium was replaced every other day.

Measurement of growth factors. Lung and adult dermal HMVECs were cultured on 12-well type I collagen–coated plates. After the cell density reached 70% confluence, the cells were further cultured for 72 hours in CS-C serum-free medium (SF-4Z0-500; Cell Systems) containing different amounts of C3f, DRC3f, and FPA (0, 15.6, 31.25, 62.5, 125, 250, and 500 ng/ml) with or without 20 ng/ml recombinant human insulin-like growth factor 1 (IGF-1) (Promega, Madison, WI). Similarly, normal human dermal fibroblasts were cultured on 12-well plates in RPMI 1640 medium containing 10% FBS. After the cell density reached 70% confluence, the cells were further cultured for 72 hours with serum-free RPMI 1640 medium containing different amounts of C3f, DRC3f, and FPA with or without IGF-1. The supernatant was collected and stored at −20°C until used.

Quantikine immunoassay kits (R&D Systems, Minneapolis, MN) were used for quantifying human transforming growth factor β1 (TGFβ1), vascular endothelial growth factor (VEGF), and epidermal growth factor (EGF). Concentrations of TGFβ1, VEGF, and EGF in the supernatants of the 3 cell lines were measured according to the manufacturer's instructions.

Cell proliferation assay. Lung and adult dermal HMVECs were cultured in growth factor–free medium on type I collagen–coated 96-well plates at a cell density of 4,000/well. Normal human dermal fibroblasts were cultured in RPMI 1640 medium containing 1% FBS at a cell density of 3,000/well. C3f, DRC3f, or FPA, variously diluted in medium, was then added into the wells with or without IGF-1. Six different wells were used for each condition to calculate the mean cell numbers.

Proliferation of lung and adult dermal HMVECs was also quantitated using, in place of synthesized peptides, whole sera or filtered serum samples that were negative or positive for DRC3f. Specifically, serum samples filtrated with a 0.2-μm filter (Millex; Millipore) were added to the culture medium up to a final concentration of 5% (5 μl per well). Similarly, serum samples filtrated with a 3.0-kd filter (Microcon; Millipore) were added into the medium up to a final concentration of 15% (15 μl per well). Cells were cultured on 96-well plates for 48 hours at 37°C in a humidified atmosphere of 5% CO_2.

The CellTiter 96 AQ_{ueous} One Solution Cell Proliferation Assay (Promega) was used for evaluating cell proliferation, according to the manufacturer's instructions. Briefly, 20 μl of CellTiter 96 AQ_{ueous} One Solution reagent was added into each well of the plate, followed by incubation for 2 hours. Absorbance at 490 nm was then measured using a 96-well microplate reader. The fold increase in mean cell number was calculated according to the formula: fold increase = mean absorbance value in a single well/mean absorbance value in unstimulated cell wells.

Statistical analysis. Levels of peptide peaks, clinical data, and age of the patients were expressed as the mean ± SD. Student's *t*-test was used for comparisons between the mean values. Chi-square test was used to evaluate differences in frequency. The relationship of DRC3f levels with clinical and laboratory data were analyzed using linear correlation analysis. Effects of stimulation by C3f and DRC3f on cell proliferation as well as on production of TGFβ1, VEGF, and EGF were expressed as the relative change from baseline (nonstimulated values), using repeated-measures analysis of variance and Student-Newman-Keuls tests for pairwise comparisons. *P* values less than 0.05 were considered significant.

RESULTS

Detection of predominant peptide peaks in SSc sera. To find disease-related peptides in sera from patients with SSc, we first purified peptides from the serum samples using MS-HIC18 magnetic beads, and then detected profiles of the purified peptides in each of the serum samples by MALDI-TOF mass spectrometry. We compared the peptide profiles between patients with

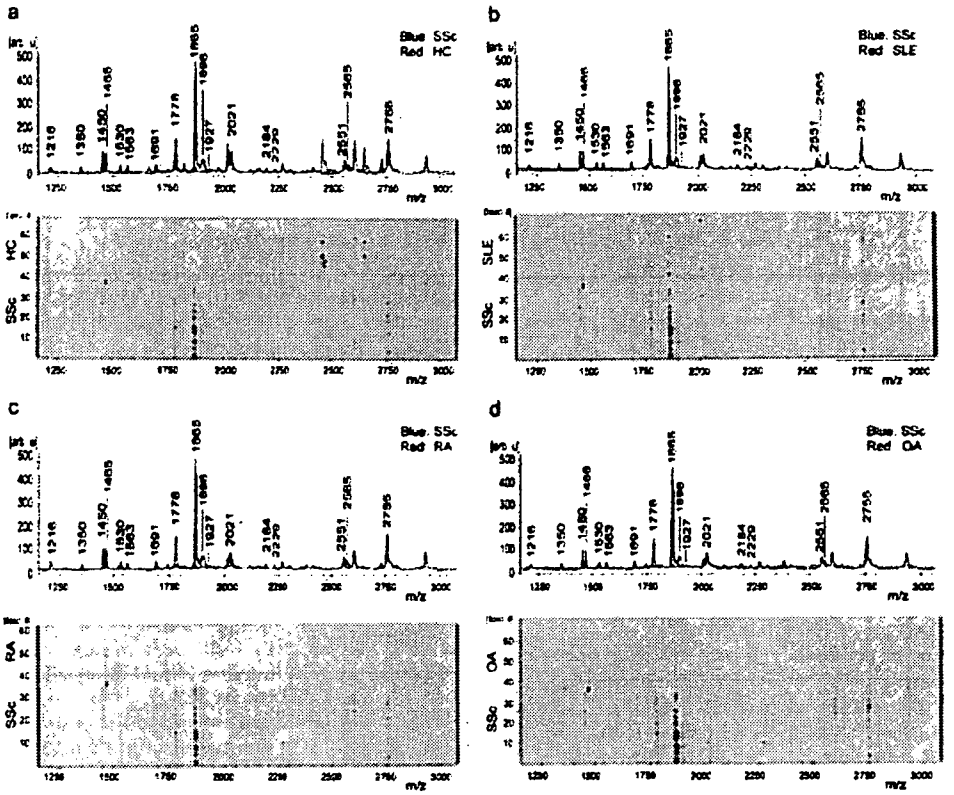

Figure 1. Spectra of serum peptide peaks in patients with systemic sclerosis (SSc) as compared with healthy controls (HC) (a), patients with systemic lupus erythematosus (SLE) (b), patients with rheumatoid arthritis (RA) (c), or patients with osteoarthritis (OA) (d). The mean peak intensities for the peptide spectra were compared using ClinPro Tools software, in 40 serum samples from SSc patients, 30 from SLE patients, 21 from RA patients, 30 from OA patients, and 26 from healthy control subjects. A range of mass/charge (m/z) values, from 1,000 daltons to 3,000 daltons, is shown. Upper panels show comparisons of the mean peak spectra between groups, with results expressed in arbitrary units (arb. u). Lower panels show the peptide peak spectra in the serum of each patient by 2-dimensional density plot in Pseudo Gel View; the peptide peak intensities were converted to a gel separation image to facilitate visualization. Spect. = spectrum.

SSc and patients with other diseases (SLE, RA, and OA), using CPT analysis. As a result, several peptide peaks, such as those with mass/charge (m/z) values of 1,865, 1,778, 1,691, 1,563, and 1,450, were detected predominantly in the SSc sera (Figure 1).

We next compared the mean peak intensity levels between patients with SSc and the other groups of patients or healthy controls. As shown in Figure 2a, the mean intensities of peptide peaks for the peptides with m/z of 1,450, 1,563, 1,778, and 1,865 were significantly higher in SSc sera than in sera from SLE, RA, and OA patients or healthy controls.

To further evaluate the levels of these peaks, we compared the frequency of peptide-positive serum samples between SSc patients and the healthy controls and patient groups by assessing each of the peptide peaks for peptides with m/z of 1,450, 1,563, 1,691, 1,778, and 1,865. As shown in Figure 2b, the frequencies of peptide-positive serum samples for peptides with m/z of 1,450, 1,563, and 1,778 were significantly higher in the SSc group than in all other groups. For peptides with m/z of 1,691 and 1,865, the frequencies of peptide-positive serum samples were significantly higher in the SSc patients than in the RA patients, OA patients, and healthy control subjects; however, the differences in these peptide frequencies between patients with SSc and

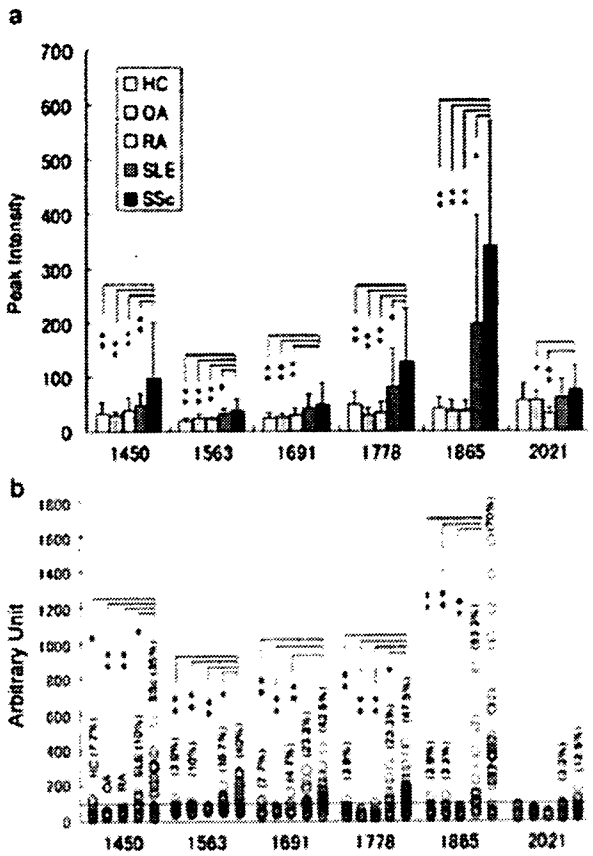

Figure 2. Genetic algorithms analysis of peptide peaks. **a,** Comparison of mean peak peptide areas between patients with SSc and the other groups, for peptide peak areas with m/z of 1,450, 1,563, 1,691, 1,778, 1,865, and 2,021, by ClinPro Tools paired analysis. **b,** Comparison of the frequency of peaks for peptides with m/z of 1,450, 1,563, 1,691, 1,778, 1,865, and 2,021 between patients with SSc and the other groups. Frequency values are shown in parentheses. The solid horizontal line indicates the cutoff point of 100 arbitrary units (the mean peak intensity + 3 SD in healthy controls). Circles indicate individual values. Broken horizontal lines indicate the mean arbitrary units for each group. * = $P < 0.05$; ** = $P < 0.01$. See Figure 1 for definitions.

patients with SLE were not statistically significant. In addition, only small differences in mean peak intensity and frequency of peptide positivity for the peptide with m/z of 2,021 were observed among the tested groups.

We then calculated the fold increase in mean peak area of these peptide peaks among the SSc, SLE, RA, and OA groups (Table 1). The results further confirmed that the increases in these peptide peaks were highest in SSc sera. In particular, the mean peak intensities for peptides with m/z of 1,865 and 1,778 in the SSc sera were >18 times as high as those in the healthy control sera. Our findings suggest that these predominant peptides could be linked to the pathophysiologic processes of SSc.

Identification of SSc-predominant peptides as derivatives of C3f. We next determined the amino acid sequences of the detected peptides by MALDI-TOF mass spectrometry, followed by a de novo sequencing method. As a result, the peptide with m/z of 1,865 was identified as DRC3f, a degraded derivative of C3f produced by removal of the C-terminal arginine with carboxypeptidase N (21). The other peptides, with m/z of 1,778, 1,691, 1,563, and 1,450, were identified as shorter derivatives of DRC3f (Table 1). We also identified the peptide with m/z of 2,021 as C3f itself. It is very interesting that the relative concentration of DRC3f and its degraded peptides, with m/z of 1,778, 1,691, 1,563, and 1,450, were much higher in the SSc group than in the other groups, whereas the relative concentration of C3f itself, with m/z of 2,021, in the SSc group did not differ substantially from that in the other groups (Table 1).

In addition to DRC3f and its degraded peptides, we identified other peptides that were detected predominantly in the SSc sera (shown in Table 1). However, the peak levels of these peptides in the sera were much lower than those of DRC3f. Therefore, in the present study, we focused solely on DRC3f.

Relationship of DRC3f to vascular involvement and disease activity in SSc. We next investigated whether the elevated levels of DRC3f (m/z 1,865) were associated with clinical features in the patients with SSc. Based on the predefined cutoff point of 100 arbitrary units (as shown in Figure 2b), we classified the patients with SSc into 2 groups according to whether their serum levels of DRC3f were elevated (DRC3f-elevated; n = 28) or were within the normal range (DRC3f-normal; n = 12). We then identified the clinical features that showed an association with elevated DRC3f levels (Table 2).

Our results revealed that disease duration was significantly longer in the DRC3f-elevated group than in the DRC3f-normal group ($P < 0.05$). Raised levels of DRC3f were observed in 12 (54.5%) of the 22 patients with a disease duration shorter than 5 years compared with 16 (88.9%) of the 18 patients with a disease duration of ≥5 years. However, among only the patients in the DRC3f-elevated group, the mean DRC3f level was higher in those with a disease duration of <5 years than in those with a disease duration of ≥5 years.

In addition, the frequencies of interstitial lung disease (ILD), symptoms of sicca syndrome, and esoph-

Table 1. Peptides identified by mass spectrometry and the fold increase in mean peak area in the sera of patients with systemic sclerosis (SSc) compared with patients with other rheumatic diseases*

Peptide m/z	Peptide family	Amino acid sequence	Amino acid position		Accession no.	Mean peak area fold increase versus healthy controls			
			Start	End		SSc	SLE	RA	OA
1,449.77	Complement C3f	THRIHWESASLL	5	16	1413205A	7.63†	2.12	1.85	0.67
1,562.86	Complement C3f	ITHRIHWESASLL	4	16	1413205A	8.56†	4.03	1.13	0.46
1,690.98	Complement C3f	KITHRIHWESASLL	3	16	1413205A	16.14‡	12.21	0.46	1.60
1,777.96	Complement C3f	SKITHRIHWESASLL	2	16	1413205A	18.13†	5.77	1.52	1.19
1,865.01	Complement C3f	SSKITHRIHWESASLL	1	16	1413205A	18.98†	7.02	1.02	0.76
2,021.11	Complement C3f	SSKITHRIHWESASLLR	1	17	1413205A	1.24‡	1.06	0.28	0.45
2,551.25	Complement C4	TLEIPGNSDPNMIPDGDFNSYVR	957	979	AAB67980	0.97	0.74	0.88	0.96
2,565.55	Complement C4	TLEIPGNSDPNMIPDGDFNSYVR+ Me-ester (DE)	957	979	AAB67980	8.54†	2.27	1.82	0.29
1,895.96	Complement C4	NGFKSHALQLNNRQIR	1,337	1,352	AAB67980	3.59§	1.76	2.44	0.27
1,530.08	Clusterin	RPHFFFPKSRIV	214	226	P10909	11.4†	2.18	2.79	0.94
2,184.08	ITIH4	QLGLPGPPDVPDHAAYHPFR	669	688	Q14624	4.94†	0.39	1.44	0.41
2,229.04	Albumin	DAHKSEVAHRFKDLGEENF	25	43	AAH39235	3.44†	1.49	1.05	0.99
1,927.86	Apolipoprotein A-IV precursor	SLAELGGHLDQQVEEFR	288	304	AAA96731	2.84‡	1.83	1.04	1.47
2,755.43	Apolipoprotein A-IV precursor	GNTEGLQKSLAELGGHLDQQVEEFR	280	304	AAA96731	5.27‡	4.48	1.15	0.81

* m/z = mass/charge; SLE = systemic lupus erythematosus; RA = rheumatoid arthritis; OA = osteoarthritis; ITIH4 = inter-α trypsin inhibitor heavy-chain H4 precursor.
† $P < 0.05$ versus SLE, RA, and OA groups.
‡ $P < 0.05$ versus RA and OA groups.
§ $P < 0.05$ versus SLE and OA groups.

ageal involvement were significantly higher in the DRC3f-elevated group than in the DRC3f-normal group (all $P < 0.05$). Interestingly, pitting scars and active digital ulcers were observed in only the DRC3f-elevated group. The frequency of use of prostaglandin I_2–maintaining therapy was also higher in the DRC3f-elevated group.

The mean titer of anticentromere antibodies, a biomarker of mild SSc, was significantly higher in the DRC3f-normal group ($P < 0.05$), whereas the mean titer of anti–topoisomerase I antibodies was significantly higher in the DRC3f-elevated group ($P < 0.05$). Patients with raised DRC3f levels had a higher mean skin thickness score, but the difference compared with patients with DRC3f levels in the normal range was not statistically significant. These results suggest that DRC3f may be associated with the diffuse form of SSc as well as with long-lasting disease and vascular involvement in SSc.

With regard to laboratory data, the DRC3f-elevated group showed decreased levels of serum C3 and C4 more frequently than did the DRC3f-normal group (Table 2) (both $P < 0.05$). Moreover, the mean concentrations of serum C3, C4, and CH50 were significantly lower in the DRC3f-elevated group than in the DRC3f-normal group (all $P < 0.05$) (Table 2). DRC3f levels were negatively correlated with the levels of C3 and C4 ($r = -0.423$ and -0.397, respectively, both $P < 0.05$) (results not shown). These findings suggest that DRC3f could be an indicator of activation of the complement system in SSc.

In addition, the concentration of CRP was higher and the ESR was more elevated in patients with raised DRC3f levels than in patients with normal-range DRC3f levels (both $P < 0.05$) (Table 2). DRC3f levels were positively correlated with the ESR ($r = 0.272$, $P < 0.05$) (results not shown).

Finally, we found that the serum IgG and IgA levels were much higher in the DRC3f-elevated group than in the DRC3f-normal group of SSc patients (Table 2). DRC3f levels were positively correlated with IgA levels ($r = 0.432$, $P < 0.05$) (results not shown). These findings suggest a role for DRC3f in SSc disease activity.

We next analyzed the relationship between DRC3f levels and disease activity in patients with SLE and patients with RA. We found that the DRC3f level was elevated in 16 patients with SLE (53.3%) (Figure 2), and that the DRC3f-elevated group of SLE patients had lower levels of serum C3 and C4 than did the DRC3f-normal group of SLE patients. However, the SLEDAI score was not correlated with DRC3f levels. In fact,

Table 2. Comparison of clinical and laboratory data between DRC3f-elevated and DRC3f-normal groups of patients with SSc*

	Total (n = 40)	DRC3f-normal (n = 12)	DRC3f-elevated (n = 28)
Clinical			
Age at disease onset, mean ± SD years	49.6 ± 10.1	54.3 ± 11.9	47.6 ± 9.2
Disease duration, mean ± SD years	6.83 ± 6.3	1.25 ± 1.202	9.21 ± 7.45†
No. female/no. male	39/1	11/1	28/0
dcSSc	18 (45)	4 (33)	14 (50)
lcSSc	22 (55)	8 (67)	14 (50)
Skin thickness score, mean ± SD	19 ± 9.15	15.6 ± 9.5	20.4 ± 8.61
Raynaud's phenomenon	37 (93)	10 (83)	27 (96)
Digital pitting scar	11 (28)	0	11 (39)†
Active digital ulcer	4 (10)	0	4 (14)
ILD	24 (60)	1 (8)	23 (82)‡
Pulmonary hypertension	1 (3)	0	1 (4)
Esophageal involvement	25 (63)	3 (25)	22 (79)†
Sicca symptoms	17 (43)	2 (17)	15 (54)†
Proteinuria	2 (5)	0	2 (7)
Anemia	8 (20)	1 (8)	7 (25)
Laboratory			
ANA positive	37 (93)	10 (83)	27 (96)
Titer, mean ± SD	1,739.7 ± 452.7	736.67 ± 452.7	2,169.6 ± 1,771.7†
Anti–topo I positive	11/36 (31)	1/36 (3)	10/36 (28)†
Titer, mean ± SD	1.6 ± 0.66	0.36 ± 0.46	2.32 ± 1.97†
Anticentromere positive	20/30 (67)	4/30 (13)	16/30 (53)†
Titer, mean ± SD	60.1 ± 86.3	108.9 ± 83.1	41.9 ± 58.4†
Anti–U1 RNP positive	8/36 (22)	0/10	8/36 (22)†
Anti-ssDNA positive	3/26 (12)	1/26 (4)	2/26 (8)
Anti-dsDNA positive	3/20 (15)	1/20 (5)	2/20 (10)
Anti-SSA positive	3/36 (8)	0/36	3/36 (8)
Anti-SSB positive	0/36	0/36	0/36
Anti-Sm positive	0/33	0/33	0/33
Anti–Jo-1 positive	0/16	0/16	0/16
RF, mean ± SD AU/ml	44.7 ± 35.4	27.58 ± 32.7	55.11 ± 54.8†
>6 AU/ml	35 (88)	8 (67)	27 (96)†
C3, mean ± SD mg/dl	90.66 ± 10.75	100.46 ± 9.59	89.71 ± 8.7†
<60 mg/dl	7 (18)	0	7 (25)†
C4, mean ± SD mg/dl	20.7 ± 3.33	24.05 ± 3.9	19.45 ± 5.59†
<15 mg/dl	7 (18)	0	7 (25)†
CH50, mean ± SD units/ml	43.2 ± 9.53	47.61 ± 9.2	41.59 ± 4.78†
>40 units/ml	29 (73)	8 (67)	21 (75)
CRP, mean ± SD mg/dl	0.75 ± 1.62	0.24 ± 0.336	0.57 ± 0.54†
>0.2 mg/dl	25 (63)	5 (42)	20 (71)
ESR, mean ± SD mm/hour	36.9 ± 19.4	26.33 ± 16.85	39.11 ± 24.42†
>30 mm/hour	20 (50)	6 (50)	14 (50)
IgG, mean ± SD mg/dl	1,898.2 ± 432.4	1,583.8 ± 432.4	2,033.03 ± 597.12†
IgA, mean ± SD mg/dl	406.2 ± 132.5	296.75 ± 132.5	453.11 ± 174.34†
IgM, mean ± SD mg/dl	183.9 ± 67.9	164.16 ± 67.9	192.39 ± 74.04
Albumin, mean ± SD gm/dl	4.21 ± 0.33	4.42 ± 0.33	4.12 ± 0.34†
Creatinine, mean ± SD mg/dl	0.57 ± 0.09	0.56 ± 0.09	0.57 ± 0.11
KL-6, mean ± SD§	540.9 ± 340.3	886.5 ± 620.2	500.5 ± 226.7
SP-D, mean ± SD§	119.1 ± 95.3	104.01 ± 58.3	125.15 ± 82.3
Treatment			
Prednisone	23 (58)	6 (50)	17 (61)
Dosage, mean ± SD mg/day	6.91 ± 4.56	8.75 ± 5.12	6.11 ± 4.1
Immunosuppressor	3 (7.5)	1 (8.3)	2 (7.1)
PGI_2	23 (58)	2 (17)	21 (75)‡
ACEI/ARB	5 (13)	1 (8)	4 (14)
NSAIDs	12 (30)	2 (17)	10 (36)

* Except where indicated otherwise, values are the number/total number (%) of patients. Patients were grouped according to whether the levels of complement C3F-des-arginine (DRC3f) were elevated or within the normal range. Groups were compared by chi-square test for frequency differences or Student's *t*-test for pairwise comparisons of mean values. dcSSc = diffuse cutaneous systemic sclerosis; lcSSc = limited cutaneous systemic sclerosis; ILD = interstitial lung disease; ANA = antinuclear antibody; anti-ssDNA = anti–single-stranded DNA; anti-dsDNA = anti–double-stranded DNA; RF = rheumatoid factor; AU = arbitrary units; CRP = C-reactive protein; ESR = erythrocyte sedimentation rate; SP-D = surfactant protein D; PGI_2 = prostaglandin I_2; ACEI/ARB = angiotensin-converting enzyme inhibitor/angiotensin II type I receptor blocker; NSAIDs = nonsteroidal antiinflammatory drugs.

† $P < 0.05$ versus DRC3f-normal group.

‡ $P < 0.02$ versus DRC3f-normal group.

§ Determined in 6 samples from the DRC3f-normal group and 9 samples from the DRC3f-elevated group.

DRC3f levels in SLE patients with a SLEDAI score >21 were lower than those observed in SLE patients with SLEDAI scores <10 or 10–20 (mean ± SD DRC3f arbitrary units 84.8 ± 15.2 in patients with a SLEDAI score >21 versus 209.4 ± 22.2 and 287.4 ± 325.31 in patients with a SLEDAI score <10 and SLEDAI scores of 10–20, respectively; both $P < 0.05$).

Among patients with RA, the levels and frequency of DRC3f were much lower than in patients with SSc or patients with SLE (Figure 2). We found no significant difference in the clinical features and RA-related laboratory findings between the DRC3f-elevated and DRC3f-normal groups of patients with RA (results not shown).

Promotion of HMVEC proliferation in vitro by DRC3f and C3f. In a previous study, the hexapeptide HWESAS, which is included in the DRC3f amino acid sequence, was found to promote mitogenic activities of IGF (22). We thus expected that DRC3f might promote cell proliferation via IGF, and thereby play a role in the pathogenesis of SSc. Because skin fibroblasts and HMVECs have been demonstrated to play crucial roles in SSc, we investigated the proliferative effects of synthesized DRC3f and C3f peptides on these cells.

We found that both DRC3f and C3f enhanced proliferation of HMVECs of both a dermal cell line and a lung cell line, in the presence and in the absence of IGF (Figures 3a and b). However, neither DRC3f nor C3f affected proliferation of normal human dermal fibroblasts, even in the presence of IGF (Figures 3a and b). In addition, DRC3f showed a stronger proliferative effect than C3f (Figure 3c). These results suggest that DRC3f and C3f promote proliferation of HMVECs, but not fibroblasts.

To confirm the above-described effect of serum DRC3f on cell proliferation, we next stimulated adult dermal and lung HMVECs with DRC3f-elevated and DRC3f-normal sera from patients with SSc, patients with SLE, and healthy donors. As a result, the DRC3f-elevated sera enhanced proliferation of both HMVEC lines to a much greater extent than did the DRC3f-normal sera (Figure 4). This result was reproduced when sera that contained only low molecular weight molecules were used. Specifically, for the latter, we filtered out and removed molecules with molecular weights larger than ~3 kd, and then checked the effects with the low molecular weight peptide–containing sera. As a result, the filtered sera from the DRC3f-elevated group still enhanced proliferation of the cells to a greater extent than did the similarly filtrated DRC3f-normal sera (Figure 4). These results suggest that DRC3f functions in a manner similar to a growth factor.

Increased production of TGFβ1 in endothelial cells by DRC3f and C3f. We next investigated whether the growth factor–like function of both DRC3f and C3f was mediated by other growth factors secreted by the DRC3f- or C3f-stimulated cells. We measured concentrations of TGFβ1, VEGF, and EGF in the supernatant of these cell lines, with or without stimulation by DRC3f and C3f. As a result, both DRC3f and C3f enhanced TGFβ1 production by adult dermal HMVECs, and the highest concentration of TGFβ1 reached was 125 ng/ml. This maximal concentration of TGFβ1 stimulated by DRC3f and C3f was consistent with the maximal proliferative response of adult dermal HMVECs (as shown in Figure 3b) ($F = 6.43$ and $F = 36.83$, respectively; both $P < 0.01$).

In contrast, DRC3f and C3f did not enhance release of TGFβ1 from lung HMVECs ($F = 0.93$ and $F = 2.08$, respectively; both $P < 0.05$) (Figure 3d). Similarly, the line of normal human dermal fibroblasts used in our experiments produced very little TGFβ1, in spite of the addition of DRC3f and C3f.

VEGF and EGF were not produced by any of the 3 cell lines, even with stimulation by DRC3f and C3f (results not shown). Thus, the positive effects of DRC3f and C3f on proliferation of lung HMVECs appeared to be independent of their effects on growth factors, even though the DRC3f- and C3f-induced proliferation of adult dermal HMVECs was dependent, at least in part, on the increase in TGFβ1 production. These findings indicate that DRC3f appears to work directly as a growth factor–like molecule and, in part, indirectly via the induction of TGFβ1.

DISCUSSION

This study is the first to comprehensively survey disease-related short peptides in patients with SSc, since there have been no efficient ways to approach this in a comprehensive manner thus far. By combining purification of short peptides with C18-bound magnetic beads and peptidomics analysis by a mass spectrometry–based technique, we successfully detected and identified a series of short peptides that exist predominantly in the sera of patients with SSc. Our findings were as follows. 1) The short peptides detected predominantly in patients with SSc as compared with those with SLE, RA, or OA and healthy donors were identified as DRC3f, a fragment produced by the inactivation process of C3b, and its degraded derivatives. 2) The relative concentration of DRC3f was related to several clinical features

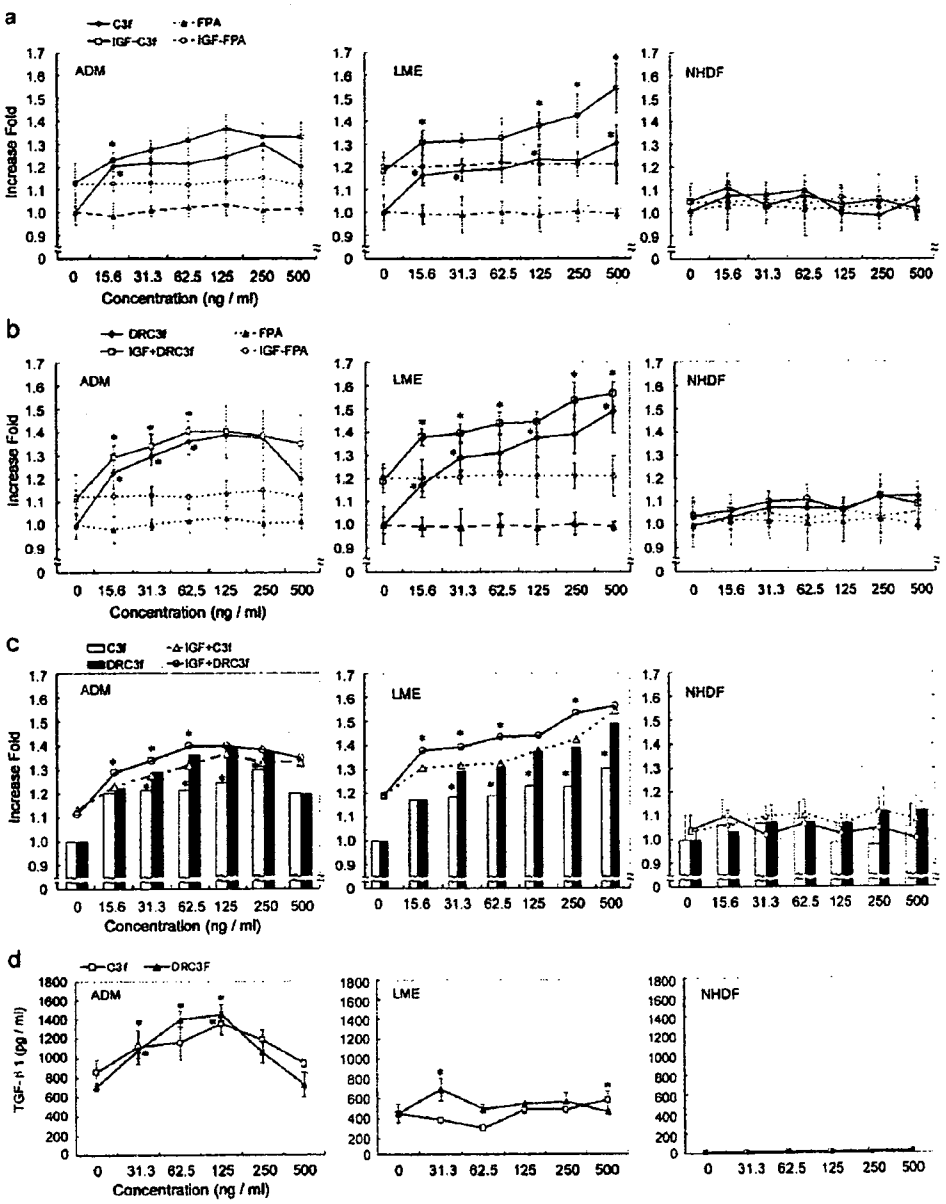

Figure 3. Influence of C3f and C3f-des-arginine (DRC3f) on cell proliferation and production of transforming growth factor β1 (TGFβ1) by normal human adult dermal microvascular endothelial cells (ADM), normal human lung microvascular endothelial cells (LME), and normal human dermal fibroblasts (NHDF). In proliferation tests, cells were cultivated in 96-well plates (3,000 cells per well) and stimulated for 48 hours with a serially diluted concentration of complement C3f (**a**) or DRC3f (**b**) in the absence or presence of insulin-like growth factor 1 (IGF-1) (20 ng/ml). Fibrinopeptide A (FPA) was used as a control. * = $P < 0.05$ between 2 adjacent concentrations of C3f or DRC3f. The influence on cell proliferation was compared between C3f and DRC3f (**c**). * = $P < 0.05$, C3f versus DRC3f stimulation with or without IGF. Values in **a**–**c** are the mean and SD fold increase in mean cell number in a single well for each concentration of stimulant (6 wells for each concentration) relative to that in unstimulated wells. To determine the influence of C3f and DRC3f on production of growth factors, the cells were cultured in 12-well plates and stimulated with different concentrations of C3f and DRC3f for 48 hours. The concentration of TGFβ1 (**d**), vascular endothelial growth factor (not shown), and epidermal growth factor (not shown) was determined in supernatants by enzyme-linked immunosorbent assay. The centrifuged supernatants of ADM and LME cells were diluted 1:4, while the supernatant of NHDFs was used directly after centrifuging without dilution. The minimum detectable dose of TGFβ1 was <7.0 pg/ml. Values in **d** are the mean and SD. * = $P < 0.05$ between 2 adjacent concentrations of C3f or DRC3f.

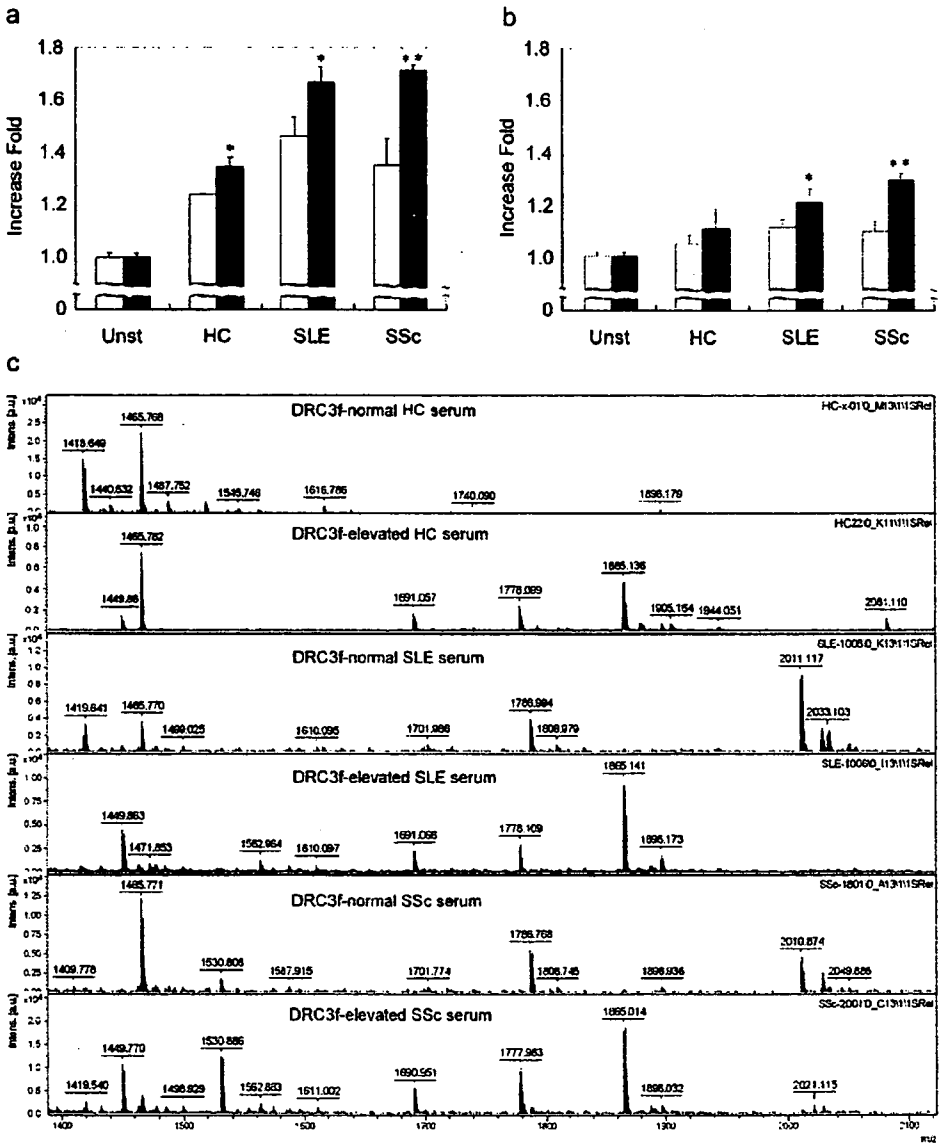

Figure 4. Proliferation of human microvascular endothelial cells (HMVECs) stimulated with either fresh or filtered sera from patients with systemic sclerosis (SSc) as compared with patients with systemic lupus erythematosus (SLE) and healthy controls (HC). Lung HMVECs (3,000 cells/well) were stimulated with fresh sera (5 μl/well) (**a**) or filtered sera (15 μl/well, filtered with a 3.0-kd filter) (**b**) from each group (n = 3 per group). Serum samples in which C3f-des-arginine (DRC3f) was in the normal range (DRC3f-normal; open bars) and serum samples in which DRC3f was detected at high levels (DRC3f-elevated; solid bars) were used to stimulate the cells. Values are the mean and SD fold increase in mean cell number relative to that in unstimulated (Unst) wells. * = $P < 0.05$; ** = $P < 0.01$ versus DRC3f-normal sera. Levels of DRC3f and its derivatives were assessed by matrix-assisted laser desorption ionization–time-of-flight (MALDI-TOF) mass spectrometry, and results were compared between DRC3f-normal and DRC3f-elevated filtered serum samples (**c**). The peptides in 3.0-kd filtered sera were separated and concentrated using Ziptip-C18 and then eluted with 50% acetonitrile. The eluate was loaded on the AnchorChip target plate and analyzed by MALDI-TOF mass spectrometry. The representative MALDI peak spectra of paired DRC3f-normal and DRC3f-elevated samples from each group are shown. The peak at mass/charge 1,865 (DRC3f) and its smaller fragments were detected in the filtered DRC3f-elevated sera, but not in the filtered DRC3f-normal sera.

and parameters of vascular involvement and disease activity in SSc. 3) Functionally, synthesized peptides of DRC3f and C3f were demonstrated to enhance proliferation of HMVECs and increase HMVEC production of TGFβ1.

The complement system has been shown to be involved in the pathogenesis of SSc. Genetically, the null allele of C4A*Q0 was reported to have a strong association with SSc (23,24). Increased serum concentrations of C1q, C2, C5, C6, C7, C9, and factor B and a decreased concentration of C4 have been observed in patients with SSc (25). Increased concentrations of C3d and C4d and increased ratios of C3d:C3 and C4d:C4 were reported to have a positive relationship with the severity of SSc (26). Another study also showed that an increased C3d level and markedly decreased complement level were dependent on prevention of immune precipitation in patients with SSc (27). In that study, immune precipitation was suppressed significantly in patients who carried the C4A*Q0 allotype (27). More recently, the activated complement complex C5b-9 and the C5a receptor were detected in the microvasculature of SSc patients, both in the early and in the late stages of the disease (28,29).

These findings suggest that both abnormal complement activation and complement heredity are involved in the pathogenesis of SSc. Activated complement may impair the membranes of endothelial cells directly by C5b-9, resulting in endothelial cell death and increased permeability of the endothelium. Furthermore, fragments released from complement activation, such as C3a and C5a, are strong chemotaxins, which attract leukocytes into sites of inflammation (30). Other fragments produced in the process of activation/inactivation of complement, such as C3b, iC3b, and C3d, may have biologic functions. However, it remains uncertain whether these degraded fragments of complement play a pathogenic role in SSc.

Complement C3 is a key molecule in the formation of C5 convertase. Complement activation includes 3 main pathways of the classical pathway, mannose-binding lectin pathway, and alternative pathway. In healthy conditions, only low-level spontaneous C3 activation occurs, via the alternative pathway. C3b, produced by C3 activation, is degraded to form inactive iC3b with the help of complement receptor 1 (CR1) or factor H, while, simultaneously, C3f of a 17-amino-acid peptide is cleaved from C3b. C3f is further degraded to form DRC3f via carboxypeptidase N, which leads to release of the C-terminal arginine, the main form of C3f derivatives (20). Thus, DRC3f might also be a marker of complement activation. In fact, our results showed that the dramatic increase in serum levels of DRC3f in SSc patients had a negative correlation with the serum C3 and C4 levels.

However, it remains unclear why the DRC3f levels were much higher in patients with SSc than in patients with SLE, the classic immune complex disease. The increased basic levels of complement components, including C3, in those with SSc might have partially contributed to elevations in the DRC3f level (25), whereas the reduced levels of complement regulators, including CR1, and quick depletion of the complement components (31) might have contributed to the lower level of DRC3f in those with SLE. It would be of value to investigate the activity of complement regulatory proteins, including CR1, factor H, and factor I, in SSc.

We found that the DRC3f level had a significant correlation with the level of IgA. In a previous study, IgA-containing immune deposits were detected at vascular sites in patients with SSc (32). Moreover, IgA in immune aggregates deposited at vascular sites was demonstrated to trigger activation of the complement cascade through the alternative pathway (33,34). Both of these features of IgA may play important pathologic roles in SSc. Functionally, both C3f and DRC3f have been demonstrated to enhance vascular permeability and induce smooth muscle contraction as a weak spasmogen (20). The hexapeptide HWESAS, a sequence encompassed within C3f, has recently been found to potentiate the sulfation and mitogenic activities of the IGFs (22). Based on these findings in addition to our own results, we hypothesized that DRC3f could play a role in the pathogenesis of SSc.

To test this point, we synthesized both C3f peptides and DRC3f peptides and observed the functions of both peptides in vitro. Our results showed that the synthesized C3f and DRC3f promoted proliferation of HMVECs independent of any role of IGF. In addition, we showed that both the DRC3f-containing serum samples and the filtered DRC3f-containing serum samples (containing only molecules with molecular weights of lower than ~3 kd) enhanced the proliferation of HMVECs (Figure 4). These results suggest that DRC3f is one of the low molecular weight growth factors in sera (22,35). However, morphologic abnormalities in the vessels, defective angiogenesis, and apoptosis instead of proliferation of endothelial cells are common features of the microvasculature in SSc. This appears to be consistent with the increased DRC3f levels observed in the present study.

In contrast with the findings in skin HMVECs, lung HMVECs have been demonstrated to proliferate in

bleomycin-induced pulmonary fibrosis in rats (36), in SSc patients with fibrosing alveolitis (37,38), and in SSc patients with pulmonary hypertension (39). We found that HMVECs from a lung cell line showed a higher frequency of proliferative responses to DRC3f and C3f than did HMVECs from a skin cell line. Moreover, the DRC3f level was associated with ILDs in patients with SSc. Thus, DRC3f may play a role in the pathogenesis of SSc in association with ILDs and/or pulmonary hypertension.

It has been demonstrated that growth factors, including TGFβ, are responsible for proliferation of dermal fibroblasts and small artery smooth muscle cells, and for excessive production of extracellular matrix components such as types I, III, V, and VII collagens and fibronectin (40). We therefore also investigated the influence of DRC3f and C3f on the production of TGFβ1, VEGF, and EGF, using the same cell lines as above. Both DRC3f and C3f markedly enhanced production of TGFβ1 by the HMVECs of a skin cell line, but not by the lung HMVECs or a human dermal fibroblast cell line. None of the 3 cell lines were found to produce detectable amounts of VEGF and EGF after stimulation with either DRC3f or C3f. Thus, in our study, DRC3f and C3f failed to show a growth factor–like potential, at least with regard to the expression of TGFβ1, VEGF, and EGF, even though a part of this potential could be attributed to expression of TGFβ1 in one of the tested cell lines. Alternatively, DRC3f and C3f may have a direct influence on HMVECs. To resolve this issue, we are currently investigating target molecules of DRC3f and C3f, using a comprehensive proteomics approach.

With regard to clinical features, the DRC3f level was associated with higher levels of antinuclear antibodies, rheumatoid factor, IgG, IgA, and CRP, lower levels of C3, C4, and CH50, an accelerated ESR, and presence of anti–topoisomerase I and anti-RNP antibodies. These findings indicate that DRC3f could be linked to pathologic immune reactions in SSc. In addition, the DRC3f level was associated with ILDs, digital pitting scars, sicca symptoms, and esophageal involvement. DRC3f therefore appears to be linked to the activity and severity of SSc, including vascular involvement. However, the DRC3f level did not correlate significantly with the modified Rodnan total skin thickness score, which is a measure of the main feature of SSc.

In addition, the level of DRC3f was associated with long disease duration, but the activity of SSc is often higher in the early stages of the disease. It is also puzzling that DRC3f levels were associated with the presence of ILDs but not with KL-6 and surfactant protein D. Therefore, we must conclude, based on the available evidence, that the linkage of DRC3f to the activity and severity of SSc might be only partial. To resolve this issue, future investigations into the mechanisms by which DRC3f contributes to the clinical features of SSc are needed.

In summary, DRC3f and its smaller derivatives, produced in the process of inactivation of C3b, were detected predominantly in the sera of patients with SSc in association with disease activity and vascular involvement. We further demonstrated DRC3f to be a low molecular weight growth factor that enhanced proliferation of HMVECs and, in some cells, enhanced TGFβ1 production. These results suggest that the activation of complement and the effects of DRC3f each play a crucial role in the pathogenesis of SSc. Future studies should focus on the functions of DRC3f in SSc sera, since this would provide us with valuable information regarding the pathophysiologic mechanisms of the disease.

ACKNOWLEDGMENTS

We thank Ms Mie Kanke and Ms Mayumi Tamaki for their technical assistance.

AUTHOR CONTRIBUTIONS

Dr. Xiang had full access to all of the data in the study and takes responsibility for the integrity of the data and the accuracy of the data analysis.

Study design. Xiang, Nakamura, Masuko, Yudoh, Nishioka, Kato.
Acquisition of data. Matsui, Matsuo, Shimada, Tohma.
Analysis and interpretation of data. Xiang, Matsui, Matsuo, Shimada, Tohma, Nakamura, Masuko, Yudoh, Nishioka, Kato.
Manuscript preparation. Xiang, Kato.
Statistical analysis. Xiang, Kato.

REFERENCES

1. Rodnan GP, Myerowitz RL, Justh GO. Morphologic changes in the digital arteries of patients with progressive systemic sclerosis (scleroderma) and Raynaud phenomenon. Medicine (Baltimore) 1980;59:393–408.
2. Pignone A, Scaletti C, Matucci-Cerinic M, Vazquez-Abad D, Meroni PL, Del Papa N, et al. Anti-endothelial cell antibodies in systemic sclerosis: significant association with vascular involvement and alveolo-capillary impairment. Clin Exp Rheumatol 1998;16:527–32.
3. Kantor TV, Friberg D, Medsger TA Jr, Buckingham RB, Whiteside TL. Cytokine production and serum levels in systemic sclerosis. Clin Immunol Immunopathol 1992;65:278–85.
4. Sato S, Hanakawa H, Hasegawa M, Nagaoka T, Hamaguchi Y, Nishijima C, et al. Levels of interleukin 12, a cytokine of type 1 helper T cells, are elevated in sera from patients with systemic sclerosis. J Rheumatol 2000;27:2838–42.
5. Sato S, Nagaoka T, Hasegawa M, Tamatani T, Nakanishi T,

Takigawa M, et al. Serum levels of connective tissue growth factor are elevated in patients with systemic sclerosis: association with extent of skin sclerosis and severity of pulmonary fibrosis. J Rheumatol 2000;27:149–54.
6. Yamane K, Miyauchi T, Suzuki N, Yuhara T, Akama T, Suzuki H, et al. Significance of plasma endothelin-1 levels in patients with systemic sclerosis. J Rheumatol 1992;19:1566–71.
7. Nordenbaek C, Johansen JS, Halberg P, Wiik A, Garbarsch C, Ullman S, et al. High serum levels of YKL-40 in patients with systemic sclerosis are associated with pulmonary involvement. Scand J Rheumatol 2005;34:293–7.
8. Sato S, Fujimoto M, Hasegawa M, Komura K, Yanaba K, Hayakawa I, et al. Serum soluble CTLA-4 levels are increased in diffuse cutaneous systemic sclerosis. Rheumatology (Oxford) 2004;43:1261–6.
9. Sato S, Komura K, Hasegawa M, Fujimoto M, Takehara K. Clinical significance of soluble CD31 in patients with systemic sclerosis (SSc): association with limited cutaneous SSc. J Rheumatol 2001;28:2460–5.
10. Feghali-Bostwick CA. Genetics and proteomics in scleroderma. Curr Rheumatol Rep 2005;7:129–34.
11. Schrader M, Schulz-Knappe P. Peptidomics technologies for human body fluids. Trends Biotechnol 2001;19 Suppl 10:S55–60.
12. Schrader M, Selle H. The process chain for peptidomic biomarker discovery. Dis Markers 2006;22:235–45.
13. Soloviev M, Finch P. Peptidomics: current status. J Chromatogr B Analyt Technol Biomed Life Sci 2005;815:11–24.
14. Subcommittee for Scleroderma Criteria of the American Rheumatism Association Diagnostic and Therapeutic Criteria Committee. Preliminary criteria for the classification of systemic sclerosis (scleroderma). Arthritis Rheum 1980;23:581–90.
15. Clements P, Lachenbruch P, Siebold J, White B, Weiner S, Martin R, et al. Inter and intraobserver variability of total skin thickness score (modified Rodnan TSS) in systemic sclerosis. J Rheumatol 1995;22:1281–5.
16. Tan EM, Cohen AS, Fries JF, Masi AT, McShane DJ, Rothfield NF, et al. The 1982 revised criteria for the classification of systemic lupus erythematosus. Arthritis Rheum 1982;25:1271–7.
17. Bombardier C, Gladman DD, Urowitz MB, Caron D, Chang DH, and the Committee on Prognosis Studies in SLE. Derivation of the SLEDAI: a disease activity index for lupus patients. Arthritis Rheum 1992;35:630–40.
18. Altman R, Asch E, Bloch D, Bole G, Borenstein D, Brandt K, et al. Development of criteria for the classification and reporting of osteoarthritis: classification of osteoarthritis of the knee. Arthritis Rheum 1986;29:1039–49.
19. Zhang X, Leung SM, Morris CR, Shigenaga MK. Evaluation of a novel, integrated approach using functionalized magnetic beads, bench-top MALDI-TOF-MS with prestructured sample supports, and pattern recognition software for profiling potential biomarkers in human plasma. J Biomol Tech 2004;15:167–75.
20. Ganu VS, Muller-Eberhard HJ, Hugli TE. Factor C3f is a spasmogenic fragment released from C3b by factors I and H: the heptadeca-peptide C3f was synthesized and characterized. Mol Immunol 1989;26:939–48.
21. Harrison RA, Farries TC, Northrop FD, Lachmann PJ, Davis AE. Structure of C3f, a small peptide specifically released during inactivation of the third component of complement. Complement 1988;5:27–32.
22. Dousset B, Straczek J, Maachi F, Nguyen DL, Jacob C, Capiaumont J, et al. Purification from human plasma of a hexapeptide that potentiates the sulfation and mitogenic activities of insulin-like growth factors. Biochem Biophys Res Commun 1998;247:587–91.
23. Briggs DC, Welsh K, Pereira RS, Black CM. A strong association between null alleles at the C4A locus in the major histocompatibility complex and systemic sclerosis. Arthritis Rheum 1986;29:1274–7.
24. Takeuchi F, Nabeta H, Hong GH, Matsuta K, Tokunaga K, Tanimoto K, et al. C4A and C4B null alleles are genetic markers of different types of systemic sclerosis in Japanese patients. Clin Exp Rheumatol 1998;16:55–60.
25. Benbassat C, Schlesinger M, Luderschmidt C, Valentini G, Tirri G, Shoenfeld Y. The complement system and systemic sclerosis. Immunol Res 1993;12:312–6.
26. Senaldi G, Lupoli S, Vergani D, Black CM. Activation of the complement system in systemic sclerosis: relationship to clinical severity. Arthritis Rheum 1989;32:1262–7.
27. Arason GJ, Geirsson AJ, Kolka R, Vikingsdottir T, Valdimarsson H. Deficiency of complement-dependent prevention of immune precipitation in systemic sclerosis. Ann Rheum Dis 2002;61:257–60.
28. Magro CM, Nuovo G, Ferri C, Crowson AN, Giuggioli D, Sebastiani M. Parvoviral infection of endothelial cells and stromal fibroblasts: a possible pathogenetic role in scleroderma. J Cutan Pathol 2004;31:43–50.
29. Sprott H, Muller-Ladner U, Distler O, Gay RE, Barnum SR, Landthaler M, et al. Detection of activated complement complex C5b-9 and complement receptor C5a in skin biopsies of patients with systemic sclerosis (scleroderma). J Rheumatol 2000;27:402–4.
30. Sallusto F, Mackay CR. Chemoattractants and their receptors in homeostasis and inflammation. Curr Opin Immunol 2004;16:724–31.
31. Ross GD, Yount WJ, Walport MJ, Winfield JB, Parker CJ, Fuller CR, et al. Disease associated loss of erythrocyte complement receptors (CR1, C3b receptors) in patients with SLE and other diseases involving autoantibodies and/or complement activation. J Immunol 1985;135:2005–14.
32. Evans DJ, Cashman SJ, Walport M. Progressive systemic sclerosis: autoimmune arteriopathy. Lancet 1987:1:480–2.
33. Schifferli JA, Steiger G, Polla L, Didierjean L, Saurat JH. Activation of the alternative pathway of complement by skin immune deposits. J Invest Dermatol 1985;85:407–11.
34. Hiemstra PS, Gorter A, Stuurman ME, Van Es LA, Daha MR. Activation of the alternative pathway of complement by human serum IgA. Eur J Immunol 1987;17:321–6.
35. Heulin MH, Rajoelina J, Artur M, Geschier C, Straczek J, Lasbennes A, et al. Isolation and characterization of a low molecular weight growth-promoting factor from human plasma. Life Sci 1987;41:297–304.
36. Kawamoto M, Fukuda Y. Cell proliferation during the process of bleomycin-induced pulmonary fibrosis in rats. Acta Pathol Jpn 1990;40:227–38.
37. Renzoni EA, Walsh DA, Salmon M, Wells AU, Sestini P, Nicholson AG, et al. Interstitial vascularity in fibrosing alveolitis. Am J Respir Crit Care Med 2003;167:438–43.
38. Fujimoto T, Matsumoto T, Shoji S. Disorganizing-fibrosing processes in alveolar walls of interstitial pneumonia, "alveolopneumonitis": a morphopathological study. Tohoku J Exp Med 1989;158:237–51.
39. Ramirez A, Varga J. Pulmonary arterial hypertension in systemic sclerosis: clinical manifestations, pathophysiology, evaluation, and management. Treat Respir Med 2004;3:339–52.
40. Postlethwaite AE. Connective tissue metabolism including cytokines in scleroderma. Curr Opin Rheumatol 1995;7:535–40.

EXTENDED REPORT

Study of active controlled monotherapy used for rheumatoid arthritis, an IL-6 inhibitor (SAMURAI): evidence of clinical and radiographic benefit from an *x* ray reader-blinded randomised controlled trial of tocilizumab

Norihiro Nishimoto, Jun Hashimoto, Nobuyuki Miyasaka, Kazuhiko Yamamoto, Shinichi Kawai, Tsutomu Takeuchi, Norikazu Murata, Désirée van der Heijde, Tadamitsu Kishimoto

Ann Rheum Dis 2007;**66**:1162–1167. doi: 10.1136/ard.2006.068064

See end of article for authors' affiliations

Correspondence to: Norihiro Nishimoto, MD, Laboratory of Immune Regulation, Graduate School of Frontier Biosciences, Osaka University 1–3, Yamada-oka, Suita, Osaka, 565-0871, Japan; norihiro@fbs.osaka-u.ac.jp

Accepted 14 April 2007
Published Online First 8 June 2007

Objective: To evaluate the ability of tocilizumab (a humanised anti-IL-6 receptor antibody) monotherapy to inhibit progression of structural joint damage in patients with RA.
Methods: In a multi-centre, *x* ray reader-blinded, randomised, controlled trial, 306 patients with active RA of <5 years' duration were allocated to receive either tocilizumab monotherapy at 8 mg/kg intravenously every 4 weeks or conventional disease-modifying antirheumatic drugs (DMARDs) for 52 weeks. Radiographs of hands and forefeet were scored by the van der Heijde modified Sharp method.
Results: Patients had a mean disease duration of 2.3 years and a disease activity score in 28 joints of 6.5 at baseline. Mean total modified Sharp score (TSS) was 29.4, which was very high despite the relatively short disease duration. At week 52, the tocilizumab group showed statistically significantly less radiographic change in TSS (mean 2.3; 95% CI 1.5 to 3.2) than the DMARD group (mean 6.1; 95% CI 4.2 to 8.0; $p<0.01$). Tocilizumab monotherapy also improved signs and symptoms. The overall incidences of AEs were 89% and 82% (serious AEs: 18% and 13%; serious infections: 7.6% and 4.1%) in the tocilizumab and DMARD groups, respectively.
Conclusion: Tocilizumab monotherapy was generally well tolerated and provided radiographic benefit in patients with RA.

Rheumatoid arthritis (RA) is a chronic inflammatory disease characterised by persistent synovitis and destruction of bone and cartilage in multiple joints.[1] Although etiological causes are still obscure, constitutive overproduction of interleukin-6 (IL-6), a pleiotropic cytokine that regulates the immune response, inflammation, hematopoiesis, and bone metabolism, is thought to play a pathological role in RA.[2] Overproduction of IL-6 augments autoimmune reaction and causes systemic inflammatory manifestations. IL-6, synergistically with IL-1β or TNFα, induces the production of vascular endothelial growth factor, a potent inducer of angiogenesis necessary to oxygenate the hyperplastic synovial tissues in the affected joints.[3] IL-6 in the presence of soluble IL-6 receptor induces osteoclast differentiation and can be responsible for joint destruction and osteoporosis associated with RA.[4 5] In fact, elevated IL-6 levels are observed in serum and synovial fluid in RA patients[6–10] and correlate with disease activity and radiological joint damage.[5 11–14] IL-6 levels also correlate with levels of matrix metalloproteinase 3,[15] which degrades the proteoglycan of cartilage and also predicts radiological progression.[15–17]

Tocilizumab, a humanised anti-IL-6 receptor (IL-6R) monoclonal antibody,[18] has been shown to improve the symptoms of RA in previous clinical trials.[19–22] However, there is no study to date that investigates the potential of tocilizumab in inhibiting joint damage and improving disability, which are also important therapeutic endpoints.

To investigate whether tocilizumab monotherapy provides radiographic and clinical benefits to active RA patients, we conducted a multi-centre, *x* ray reader-blinded, randomised, controlled study.

METHODS

Patients

Eligible patients were age >20 years and fulfilled the American College of Rheumatology (ACR; formerly, the American Rheumatism Association) 1987 revised criteria for the classification of RA,[23] with a disease duration of ≥6 months and <5 years. In addition, they had ≥6 tender joints (of 49 evaluated), ≥6 swollen joints (of 46 evaluated), an erythrocyte sedimentation rate (ESR) of ≥30 mm/h and C-reactive protein (CRP) of ≥20 mg/l. All candidates had an inadequate response to at least one disease modifying antirheumatic drug (DMARD) or immunosuppressant. Use of anti-TNF agents and leflunomide were not allowed within 3 months prior to the first dose. Change in dose and type of DMARDs and/or immunosuppressants, plasma exchange therapies and surgical treatments were not allowed within 4 weeks. Oral corticosteroids (prednisolone, ≤10 mg per day) were allowed if the dosage had not been changed within 2 weeks. Eligible patients had white blood cell counts of at least 3.5×10^9/l, lymphocyte counts of at least 0.5×10^9/l and platelet counts of at least 100×10^9/l at enrolment. Patients were excluded if they had a medical history of a serious allergic reaction, significant concomitant diseases, or an active intercurrent infection requiring medication within 4 weeks before the first dose. Sexually active premenopausal women were required to have a negative urine pregnancy test at the entry and to use effective contraception during the study period.

Study protocol

This study was conducted at 28 sites in Japan. The study protocol was approved by the Ministry of Health, Labor and